nature communications

Article

https://doi.org/10.1038/s41467-024-48161-z

Nitrous oxide respiration in acidophilic methanotrophs

Received: 3 January 2024

Accepted: 22 April 2024

Published online: 18 May 2024

Check for updates

Samuel Imisi Awala[1,2,9], Joo-Han Gwak[1,9], Yongman Kim[1], Man-Young Jung[3,4,5], Peter F. Dunfield[6], Michael Wagner[7,8] & Sung-Keun Rhee[1]

Aerobic methanotrophic bacteria are considered strict aerobes but are often highly abundant in hypoxic and even anoxic environments. Despite possessing denitrification genes, it remains to be verified whether denitrification contributes to their growth. Here, we show that acidophilic methanotrophs can respire nitrous oxide (N_2O) and grow anaerobically on diverse non-methane substrates, including methanol, C-C substrates, and hydrogen. We study two strains that possess N_2O reductase genes: *Methylocella tundrae* T4 and *Methylacidiphilum caldifontis* IT6. We show that N_2O respiration supports growth of *Methylacidiphilum caldifontis* at an extremely acidic pH of 2.0, exceeding the known physiological pH limits for microbial N_2O consumption. *Methylocella tundrae* simultaneously consumes N_2O and CH_4 in suboxic conditions, indicating robustness of its N_2O reductase activity in the presence of O_2. Furthermore, in O_2-limiting conditions, the amount of CH_4 oxidized per O_2 reduced increases when N_2O is added, indicating that *Methylocella tundrae* can direct more O_2 towards methane monooxygenase. Thus, our results demonstrate that some methanotrophs can respire N_2O independently or simultaneously with O_2, which may facilitate their growth and survival in dynamic environments. Such metabolic capability enables these bacteria to simultaneously reduce the release of the key greenhouse gases CO_2, CH_4, and N_2O.

Anthropogenic emissions of greenhouse gases (GHGs)—primarily carbon dioxide (CO_2), methane (CH_4), and nitrous oxide (N_2O)—are responsible for a historically rapid increase in Earth's average annual temperature of more than 0.2 °C per decade[1,2]. In addition to achieving net-zero CO_2 emissions by 2050, significant reductions in the emissions of other GHGs including CH_4 and N_2O are now critically needed. Compared to CO_2, the warming effect of CH_4 is around 28 to 34 times greater[3,4]. However, its much shorter mean lifetime of approximately 12–13 years[5] provides an additional opportunity to mitigate future climate change. Like CO_2, N_2O—the third most important GHG—has a long half-life (roughly 120 years) in the atmosphere[6], and its warming potential is about 300 times greater than CO_2 over a 100-year time scale[1]. In addition, N_2O is a major cause of ozone depletion in the stratosphere[7,8].

[1]Department of Biological Sciences and Biotechnology, Chungbuk National University, 1 Chungdae-ro, Seowon-Gu, Cheongju 28644, Republic of Korea. [2]Center for Ecology and Environmental Toxicology, Chungbuk National University, 1 Chungdae-Ro, Seowon-Gu, Cheongju 28644, South Korea. [3]Interdisciplinary Graduate Programme in Advance Convergence Technology and Science, Jeju National University, Jeju, Republic of Korea. [4]Department of Science Education, Jeju National University, Jeju, Republic of Korea. [5]Jeju Microbiome Center, Jeju National University, Jeju, Republic of Korea. [6]Department of Biological Sciences, University of Calgary, 2500 University Dr. NW, Calgary, AB T2N 1N4, Canada. [7]Division of Microbial Ecology, Department of Microbiology and Ecosystem Science, Centre for Microbiology and Environmental Systems Science, University of Vienna, Althanstrasse 14, A-1090 Vienna, Austria. [8]Department of Chemistry and Bioscience, Center for Microbial Communities, Aalborg University, Fredrik Bajers Vej 7H, 9220 Aalborg, Denmark. [9]These authors contributed equally: Samuel Imisi Awala, Joo-Han Gwak. e-mail: rhees@chungbuk.ac.kr

Although human activities are by far the most important reason for the unprecedented rise in atmospheric GHGs[9], microbial activities also play a direct role in this rise[10,11]. GHG net accumulation is regulated by the biogeochemical source-sink dynamics of GHGs exchanged between terrestrial, marine, and atmospheric reservoirs[9]. GHG production and consumption in both natural and anthropogenic ecosystems are driven primarily by microbes[10,12]. Methane fluxes in natural environments are controlled by activities of methane-producing (methanogenic) and methane-consuming (methanotrophic) microorganisms. It is estimated that 69% of the atmospheric CH_4 budget originates from microbial activities (methanogenesis) while about 50–90% of the produced CH_4 is oxidized by methanotrophs before reaching the atmosphere[13,14].

Microbes can oxidize methane under aerobic and anaerobic conditions. Aerobic methanotrophs oxidize methane to methanol by employing either particulate methane monooxygenases (pMMO) or soluble methane monooxygenases (sMMO)[15]. There are two ways in which aerobic methanotrophs use molecular oxygen (O_2): as the terminal electron acceptor of aerobic respiration and for methane activation via the methane monooxygenase[15]. Under strictly anoxic conditions, anaerobic methanotrophic microorganisms mitigate CH_4 emissions by oxidizing methane with alternative terminal electron acceptors including NO_3^-, Fe^{3+}, Mn^{4+}, SO_4^{2-}, and humic acid using reverse methanogenesis pathways[16–19]. Furthermore, intra-aerobic metabolism in the nitrite-dependent anaerobic methane-oxidizing bacterium '*Candidatus* Methylomirabilis oxyfera' using pMMO was reported[20].

Interestingly, the genomes of some aerobic methanotrophs encode denitrification enzymes including nitrate (NO_3^-), nitrite (NO_2^-), nitric oxide (NO), and N_2O reductases[21–24]. Surprisingly, however, none of the methanotroph genomes or MAGs known to date encode a complete set of denitrification genes (Supplementary Dataset 1). Kits and colleagues[21,22] demonstrated that some aerobic methanotrophs can couple NO_3^- and NO_2^- reduction to the oxidation of methane and other electron donors, including methanol, formaldehyde, formate, ethane, ethanol, and ammonia in suboxic conditions. However, whether these aerobic methanotrophs are capable of anaerobic growth with NO_3^- and NO_2^- as terminal electron acceptors remain to be seen.

More than two-thirds of N_2O emissions arise from bacterial and fungal denitrification and nitrification processes in soils[25,26]. N_2O emissions are a major concern in acidic environments due to the high production of N_2O via abiotic reactions and the inhibition of biological N_2O reduction[27,28]. Although multiple sources of N_2O exist[25], there is only one known sink for N_2O in the biosphere—the microbial reduction of N_2O to N_2, catalyzed by a copper-dependent enzyme, N_2O reductase (N_2OR) encoded by *nosZ*[29]. The NosZ enzymes found in prokaryotes are phylogenetically classified into two clades: the canonical NosZ (clade I NosZ), found mostly in denitrifiers[30], and the recently described *c*NosZ (clade II NosZ)[31], which has an additional *c*-type heme domain at the C terminus, found commonly in non-denitrifiers[31,32]. Thus, bacteria and archaea harboring the *nosZ*-type genes, in particular those classified as incomplete- or non-denitrifiers because they do not encode the full denitrification pathway, are receiving increasing attention in the search for technologies to combat N_2O emissions[32]. Previous studies have reported the presence of the *nosZ* gene in the aerobic methanotrophs, *Methylocystis* sp. SC2 (ref. 23) and *Methylocella tundrae*[24]. Further genomic analysis from this study suggests that this enzyme is present in some other aerobic methanotrophs, too (Supplementary Dataset 1). Pure culture studies have unequivocally shown that denitrifiers can grow by respiring N_2O (refs. 33,34). Moreover, an electron sink/spill role for N_2OR has been proposed for *Gemmatimonas aurantiaca* T-27 (ref. 35) without biomass production (i.e., growth). Despite the presence of N_2OR in *Methylocystis* sp. SC2, its ability to grow in anoxia under N_2O-reducing conditions is unverified[36]. Thus, the ability to grow by converting N_2O to N_2 has not yet been reported for any of the known aerobic or anaerobic methanotrophs, even with non-methane substrates such as methanol.

Methanotrophs using MMO enzymes are considered to be obligate aerobes. Paradoxically, however, they are often detected at high relative abundance in extremely hypoxic and even anoxic zones of peat bogs, wetlands, rice paddies, forest soils, and geothermal habitats[37,38]. It is therefore critical to investigate the ability of aerobic methanotrophs to use N_2O as the sole terminal electron acceptor for energy conservation and biomass production, a metabolic trait that could allow them to thrive in these anoxic ecosystems. Here, we used a multi-faceted approach to investigate the role of N_2O respiration in defining the physiology and ecology of selected aerobic methanotrophs. Growth experiments demonstrated that the presence of N_2OR in an acidophilic proteobacterial methanotroph, *Methylocella tundrae* T4, and an extremely acidophilic verrucomicrobial methanotroph, *Methylacidiphilum caldifontis* IT6, enables these organisms to respire N_2O and to produce biomass while oxidizing a wide variety of electron donors, including methanol, acetol, pyruvate, and hydrogen. In contrast to N_2O, respiration of NO_3^- and NO_2^- did not support anaerobic growth of these methanotrophs on C1 substrates. We also demonstrate that *Methylocella tundrae* T4 can reduce both O_2 and N_2O simultaneously, allowing it to oxidize more CH_4 and generate more biomass under O_2-limiting conditions. Our findings significantly expand the potential ecological niche of aerobic methanotrophs and reveal that some methanotrophic microbial strains could be used to mitigate multiple GHG emissions.

Results and discussion

N_2OR-encoding genes in aerobic methanotrophs

To identify methanotrophs capable of using N_2O as an alternative electron acceptor, publicly available genomes and metagenome-assembled genomes (MAGs) of methanotrophs were screened for *nosZ* genes. We found genes encoding N_2OR in genomes and MAGs of methanotrophs from three bacterial phyla: *Pseudomonadota*, *Verrucomicrobiota*, and *Gemmatimonadota* (Supplementary Dataset 1). They were confined to the alphaproteobacterial methanotrophs and absent in gammaproteobacterial methanotrophs in the case of the phylum *Pseudomonadota* and represented by only two genera, *Methylocella* and *Methylocystis*, which also accounted overall for the majority of the methanotroph genomes encoding *nosZ*. Similarly, *nosZ* genes were exclusively found in one representative genome in each of the phyla *Verrucomicrobiota* (represented by the genus *Methylacidiphilum*) and *Gemmatimonadota* (represented by the candidate genus 'Methylotropicum'), respectively. Phylogenetic analysis of predicted NosZ protein sequences revealed that those found in *Methylocella* and *Methylocystis* are from the clade I NosZ lineage, while those found in *Methylacidiphilum* and '*Ca*. Methylotropicum' are from the clade II NosZ lineage (Fig. 1, Supplementary Fig. 1).

Three *Methylocella tundrae* strains: T4 (re-sequenced genome), PC1 (ref. 39), and PC4 (ref. 39), have *nos* gene clusters (NGC) (Fig. 1). These are incorporated into *nosRZDFYLX* operons in strains PC4 and T4 and a *nosZDFYLX* operon in strain PC1 (Fig. 1). Strain PC1 has truncated *nosZ* and missing *nosR* genes. This is most likely due to its genome being highly fragmented into several small contigs containing missing and truncated genes. The NGC composition and operon arrangement, n*osRZDFYLX*, were largely similar in the genomes of the six N_2OR-containing *Methylocystis* species (Fig. 1), including *Methylocystis* sp. SC2 (ref. 23), *Methylocystis echinoides* LMG27198, three in-house *Methylocystis echinoides*-like isolates (strains IM2, IM3, and IM4), and a metagenome-assembled genome (MAG) of a *Methylocystis* sp. AWTPI-1 recovered from a water treatment facility[40]. A notable feature in their NGC organization was the absence of the gene encoding the membrane-anchored copper chaperon, NosL, which is primarily involved in Cu(I) delivery to apo-NosZ[41]. Methanotrophs with pMMO usually possess multiple copper chaperones[42] that may complement

NosL, making it non-essential for NosZ maturation. Altogether, the NGC in these alphaproteobacterial methanotrophs has a similar organization to those of clade I N_2O-reducers (Fig. 1). BLAST results further revealed that the individual *nos* genes in the *Methylocella* and *Methylocystis* strains shared a high degree of similarity to each other and other non-methanotrophic *Alphaproteobacteria* (Supplementary Dataset 2). Also, their NosZ proteins share high homology with proteins annotated as twin-arginine translocation (Tat)-dependent N_2OR (35–89%) and also possess the Tat signal peptide with a characteristic SRRx[F | L] motif[43] found in clade I NosZ[32].

The NGC in the genome of *Methylacidiphilum caldifontis* IT6 (ref. 44), comprises a *nosCZBLDFYC* operon (Fig. 1) but lacks the typical *nosX* and *nosR* found in clade I N_2O-reducers[31,32], involved in NosR maturation[45] and electron transfer to NosZ[46], respectively. Notably, the NGC (IT6_00904–11) was found within the cluster of genes (IT6_00903, IT6_00912–7) encoding alternative complex III (refer to Source Data for annotation information). Both the aa_3-type and cbb_3-type cytochrome *c* oxidase-encoding genes are also located next to these genes. Genes encoding two *c*-type cytochromes (*nosC*) within the *nos* operon (Fig. 1) could serve electron transport functions[47]. Interestingly, BLAST and synteny analyses of the NGC show that the individual genes are most closely related to genes found in genomes of extremely thermophilic *Hydrogenobacter* species of the phylum *Aquificota* (amino acid identities of 72.41–91.96%) (Supplementary Dataset 2) with a similar genetic organization (Fig. 1). Strain IT6 NosZ shares high similarities to proteins annotated as Sec-dependent N_2OR (35–89%) with an N-terminal Sec-type signal peptide found in clade II NosZ[31,32]; the highest identities (79–89%) were with NosZ proteins from other *Hydrogenobacter* species. *Hydrogenobacter thermophilus* TK-6, a hydrogen-oxidizing bacterium, can completely denitrify NO_3^- to N_2 gas[48], indicating the presence of a functional N_2OR. As a result, *Methylacidiphilum caldifontis* IT6 may also have a functional N_2OR due to the high similarity of its NGC to those of *Hydrogenobacter* species. Although genomes of other *Methylacidiphilum* species, including *Methylacidiphilum fumariolicum*, lacked the gene encoding the N_2OR catalytic subunit, NosZ, some genes encoding Nos accessory proteins were found (Supplementary Dataset 2). Interestingly, the N_2OR genes for *Methylacidiphilum caldifontis* IT6 were found in a genomic island (Supplementary Dataset 3) and were most likely acquired through horizontal gene transfer, which is consistent with its NosZ phylogeny (Fig. 1, Supplementary Fig. 1). This is not surprising since many key metabolic genes in verrucomicrobial methanotrophs, including those encoding the MMO, are believed to have been acquired through horizontal gene transfer[49]. As a result, *Methylacidiphilum fumariolicum* strains might have acquired the NGC before losing the key functional genes but retaining some of the accessory genes. Finally, we found a *nosZBDF* operon in the MAG of the uncultured methanotrophic bacterium '*Ca*. Methylotropicum kingii'[50] that resembles clade II NGC, with

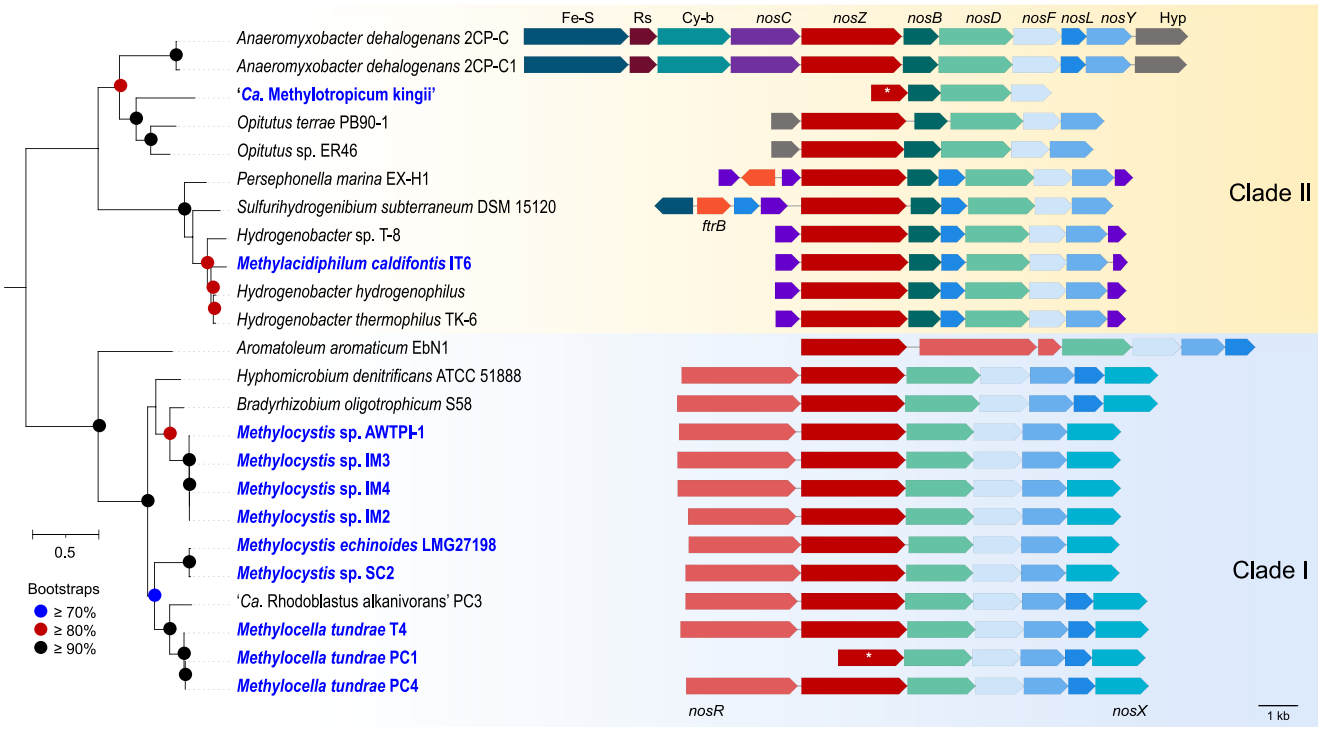

Fig. 1 | Maximum-likelihood phylogenetic tree of derived NosZ proteins, with *nos* operon arrangements in methanotrophic and non-methanotrophic bacterial strains. The phylogenetic tree was constructed with IQ-TREE (IQ-TREE options: -B 1000 -m LG + F + R5) using aligned NosZ (details in *Materials and Methods*) and rooted at the mid-point. Bootstrap values ≥ 70% based on 1000 replications are indicated. The scale bar represents a 0.5 change per amino acid position. Organization of the *nos* operon in methanotrophic strains (labeled in blue text) and closely related non-methanotrophic bacteria are shown. The genes, represented by arrows, are drawn to scale. Homologs are depicted in identical colors. The NosZ amino acid sequences and gene arrangement information were retrieved using the following genome accessions: GCF_017310505.1, *Methylacidiphilum caldifontis* IT6; GCF_000010785.1, *Hydrogenobacter thermophilus* TK-6; GCF_011006175.1, *Hydrogenobacter* sp. T-8; GCF_900215655.1, *Hydrogenobacter hydrogenophilus* DSM 2913; GCF_000619805.1, *Sulfurihydrogenibium subterraneum* DSM 15120; GCF_000021565.1, *Persephonella marina* EX-H1; GCF_000022145.1, *Anaeromyxobacter dehalogenans* 2CP1; GCF_000013385.1, *Anaeromyxobacter dehalogenans* 2CP-C; GCF_003054705.1, *Opitutus* sp. ER46; GCF_000019965.1, *Opitutus terrae* PB90-1; GCF_901905185.1, *Methylocella tundrae* PC4; GCA_901905175.1, *Methylocella tundrae* PC1; CP139089.1, *Methylocella tundrae* T4; FO000002.1, *Methylocystis* sp. SC2; GCF_000025965.1, *Aromatoleum aromaticum* EbN1; GCF_022760775.1, '*Candidatus* Rhodoblastus alkanivorans' PC3; GCF_000143145.1, *Hyphomicrobium denitrificans* ATCC 51888; GCF_000344805.1, *Bradyrhizobium oligotrophicum* S58; GCF_027923385.1, *Methylocystis echinoides* LMG27198; GCA_003963405.1, *Methylocystis* sp. AWTPI-1. * indicates that the *nosZ* genes are truncated due to genome fragmentation. Source Data contains genome annotation information for *Methylocella tundrae* T4, *Methylacidiphilum caldifontis* IT6, *Methylocystis* spp. (strains IM2, IM3, and IM4), and '*Ca*. Methylotropicum kingii'.

a truncated *nosZ* and multiple missing genes like *nosY*, *nosL*, and *nosC* (Fig. 1). These are also likely the result of multiple MAG fragmentations. Multiple sequence alignments of the predicted NosZ proteins of methanotrophs and other microorganisms (clade I and II) were constructed. All the expected metal-binding residues present in N_2OR were mostly conserved in the methanotroph NosZ sequences (Supplementary Fig. 2, Supplementary Note 1).

N_2O-dependent anaerobic growth of methanotrophs

The presence of genes predicted to encode N_2OR in the genomes of *Methylocella tundrae* strains, *Methylacidiphilum caldifontis* IT6, and *Methylocystis* strains (SC2, IM2, IM3, and IM4) (Supplementary Datasets 1, 2) led us to investigate whether this enzyme can support the anaerobic growth of these aerobic methanotrophs when N_2O is supplied as their sole electron acceptor. Physiological studies on N_2O reduction by methanotrophs focused on *Methylocella tundrae* T4 and *Methylacidiphilum caldifontis* IT6 since preliminary experiments showed that the N_2OR-containing *Methylocystis* strains, including *Methylocystis* sp. SC2 and the in-house *Methylocystis* strains (IM2, IM3, and IM4) failed to reduce N_2O under various anoxic growth conditions. We set up anoxic batch cultures of *Methylocella tundrae* T4 and *Methylacidiphilum caldifontis* IT6 using methanol as a sole electron donor with or without N_2O as the sole electron acceptor. For these incubations, 2 mM ammonium (NH_4^+) was used as the nitrogen source instead of NO_3^- to avoid the involvement of dissimilatory nitrate reduction particularly in the *Methylocella* strains with nitrate-reducing potential. As a negative control, closely related methanotrophs lacking a predicted N_2OR (*Methylocella silvestris* BL2 and *Methylacidiphilum infernorum* IT5, respectively) were included in the study design. The growth experiments were conducted in LSM medium at pH 5.5 for *Methylocella* species (strains T4 and BL2) and at pH 2.0 for *Methylacidiphilum* species (strains IT5 and IT6). As expected, in control incubations provided with O_2 as the terminal electron acceptor, all four strains grew on CH_3OH (Fig. 2A, D, G, J). In these controls, the maximum specific growth rates (μ_{max}) of the *Methylocella* strains (strain T4: $\mu_{max} = 2.83 \pm 0.03\ d^{-1}$; strain BL2: $\mu_{max} = 1.79 \pm 0.05\ d^{-1}$) were higher than those of the *Methylacidiphilum* strains (strain IT6: $\mu_{max} = 1.57 \pm 0.04\ d^{-1}$; strain IT5: $\mu_{max} = 1.49 \pm 0.01\ d^{-1}$).

Under N_2O-containing anoxic conditions, *Methylocella tundrae* T4 and *Methylacidiphilum caldifontis* IT6 reduced N_2O and grew on methanol (Fig. 2B, H). When N_2O was depleted, the growth of strains T4 and IT6 ceased. To verify that OD_{600} measurements indicated anaerobic cell growth rather than an artifact such as exopolysaccharide production, we demonstrated that cell counts and counts of 16S rRNA genes increased in parallel with OD_{600} during anaerobic growth (Supplementary Fig. 3). No growth was observed in N_2O-free anoxic conditions used as negative controls (Fig. 2C, I). These results demonstrate that the anaerobic growth of these methanotrophs was dependent on N_2O as the sole electron acceptor. The observed N_2O reduction was catalyzed by a functional respiratory N_2OR, as the N_2OR-lacking relatives (*Methylacidiphilum infernorum* IT5 and *Methylocella silvestris* BL2) used as negative controls did not grow or reduce N_2O under anoxic conditions (Fig. 2E, F, K, L). In addition, other known electron donors of *Methylocella tundrae* T4 and *Methylacidiphilum caldifontis* IT6, which support their aerobic growth[44,51,52], also supported their growth under anoxic N_2O-reducing conditions (Supplementary Dataset 4). *Methylocella tundrae* T4 grew on pyruvate and acetol, while *Methylacidiphilum caldifontis* IT6 grew on acetol under anoxic N_2O-reducing conditions. Further, molecular hydrogen supported the chemolithoautotrophic growth of *Methylacidiphilum caldifontis* IT6 as the sole electron donor under anoxic N_2O-reducing conditions (Supplementary Fig. 4). The transcriptomic analysis (see below) suggests that the group 1d [NiFe] hydrogenase encoded in the genome of *Methylacidiphilum caldifontis* IT6 could be involved in chemolithoautotrophic growth under anoxic N_2O respiring conditions.

Methylocella tundrae T4 exhibited a higher growth rate ($\mu_{max} = 0.47 \pm 0.02\ d^{-1}$) than *Methylacidiphilum caldifontis* IT6 ($\mu_{max} = 0.18 \pm 0.01\ d^{-1}$) on methanol and N_2O. However, these values are approximately 6 and 9 times, respectively, lower than the growth rates measured for both strains under O_2–respiring conditions. Biomass yields $Y_{x/m}$ (g DW·mol^{-1} N_2O or O_2 reduced) for the methanol-oxidizing cultures of strains T4 and IT6 reducing N_2O as the sole electron acceptor were also lower than for cells reducing O_2 as the sole electron acceptor. The biomass yield of *Methylocella tundrae* T4 cells grown anaerobically on N_2O (4.64 ± 0.04 g DW·mol^{-1} N_2O reduced) was approximately 45% of that of aerobically grown cells (10.41 ± 0.04 g DW·mol^{-1} O_2 reduced). Similarly, *Methylacidiphilum caldifontis* IT6 had a biomass yield when grown anoxically on N_2O (2.36 ± 0.04 g DW·mol^{-1} N_2O reduced), which was only about 38% of that achieved by aerobically grown cells (6.27 ± 0.14 g DW·mol^{-1} O_2 reduced). This improved molar yield on O_2 is expected despite the higher reduction potential of N_2O (see Eqs. [1] and [2]), since O_2 respiration accepts twice as many electrons as N_2O respiration (Eq. 1 and 2)[53]. In addition, the aerobic terminal oxidases of both strains are proton pumps and conserve energy (Supplementary Datasets 5, 6)[54,55], whereas N_2OR does neither[56]. To our knowledge, our results constitute the first report of N_2O reduction coupled with anaerobic growth in any methanotroph.

$$N_2O + 2H^+ + 2e^- \rightarrow N_2 + H_2O\ E_{0'}(\text{pH}7.0) = +1.36\text{V} \quad (1)$$

$$O_2 + 4H^+ + 4e^- \rightarrow 2H_2O + H_2O\ E_{0'}(\text{pH}7.0) = +0.82\text{V} \quad (2)$$

It is well known that N_2O reduction is generally inhibited at acidic pH (<6.0)[57], resulting in N_2O accumulation in acidic environments[28,58]. However, the current study revealed that two acidophilic methanotrophs, *Methylocella tundrae* T4 and *Methylacidiphilum caldifontis* IT6 can reduce N_2O in moderately acidic (pH 5.5) and extremely acidic (pH 2.0) conditions, respectively. The existence of acid-tolerant N_2O reducers (pH 4.0 to 6.0) has been proposed in soil microcosm and enrichment experiments[59,60]. So far, the only isolate implicated in N_2O reduction at an acidic pH (5.7) is *Rhodanobacter* sp. C01 isolated from acidic soil in Norway[61]. Our study reveals that N_2O reduction can occur even at an extremely acidic pH of 2.0. Furthermore, the conditions required for N_2O reduction in the N_2OR-containing *Methylocystis* strains remain unresolved. Perhaps some unknown growth or environmental factors are required to stimulate N_2O respiration in these methanotrophs, which will require further investigation.

Nitrate and nitrite reduction in *Methylocella* species

No anoxic growth of *Methylocella* species with CH_3OH and NO_3^-. We next tested if the presence of denitrification enzymes in *Methylocella tundrae* T4 (nitrate reductase [NAR], nitric oxide reductase [NOR] and N_2OR) and *Methylocella silvestris* BL2 (NAR, nitrite reductase [NIR], and NOR) (Supplementary Dataset 1) can equate to growth when NO_3^- or NO_2^- is used as the sole terminal electron acceptor. Indeed, the presence of NAR (and NIR) in these methanotrophs resulted in NO_3^- (and NO_2^-) reduction when methanol was provided as the sole electron donor. However, growth was barely detected under these conditions (Fig. 3A, B). Strain T4, which lacks a canonical NIR, reduced all the provided NO_3^- stoichiometrically to NO_2^- when provided with methanol as the sole electron donor (Fig. 3A). Under the same condition, strain BL2, a NAR and NIR-containing methanotroph, initially reduced the provided NO_3^- to NO_2^- and eventually, all the accumulated NO_2^- was stoichiometrically reduced to N_2O towards the end of the incubation (Fig. 3B). These results demonstrate that these methanotrophs have a functional NAR and or NIR and can utilize NO_3^- and/or NO_2^- instead of O_2 as a terminal electron acceptor. Nevertheless, these methanotrophs do not appear to rely on these activities for growth.

https://doi.org/10.1038/s41467-024-48161-z

Likewise, other aerobic methanotrophs have demonstrated denitrification activities under suboxic conditions. For example, the gammaproteobacterial methanotrophs *Methylomonas denitrificans* FJG1 and *Methylomicrobium album* BG8 were discovered to couple the oxidation of diverse electron donors to NO_3^- and NO_2^- reduction, respectively[21,22]. However, none of these strains was demonstrated to couple this activity to growth, prompting us to investigate the possible reasons behind the lack of growth (see below). It should be noted that the genomes of all known *Methylacidiphilum* strains lack genes encoding a respiratory NAR (Supplementary Dataset 1).

Toxicity of reactive nitrogen species for *Methylocella* species. Considering that methanol oxidation was coupled to N_2O reduction and led to obvious growth in the N_2OR-containing methanotrophs (Figs 2B, H), the lack of growth during NO_3^- reduction by these microorganisms is suspected to be caused by the accumulation of growth-arresting reactive nitrogen species (RNS) like NO_2^- and NO (refs. 62,63). Consistent with this hypothesis, the accumulation of NO_2^- in suboxic cultures of *Vibrio cholerae* and other bacterial species was found to limit population expansion but nitrate reduction still promoted cell viability[64]. NO_2^- typically accumulates due to a lack of functional NIR as observed for strain T4 (Fig. 3A) and, to some degree, even transiently accumulates in the presence of a functional NIR, as observed for strain BL2 (Fig. 3B). The impact of NO_2^- accumulated from NO_3^- reduction might be more severe in acidic environments since protonation of NO_2^- leads to the formation of free nitrous acid

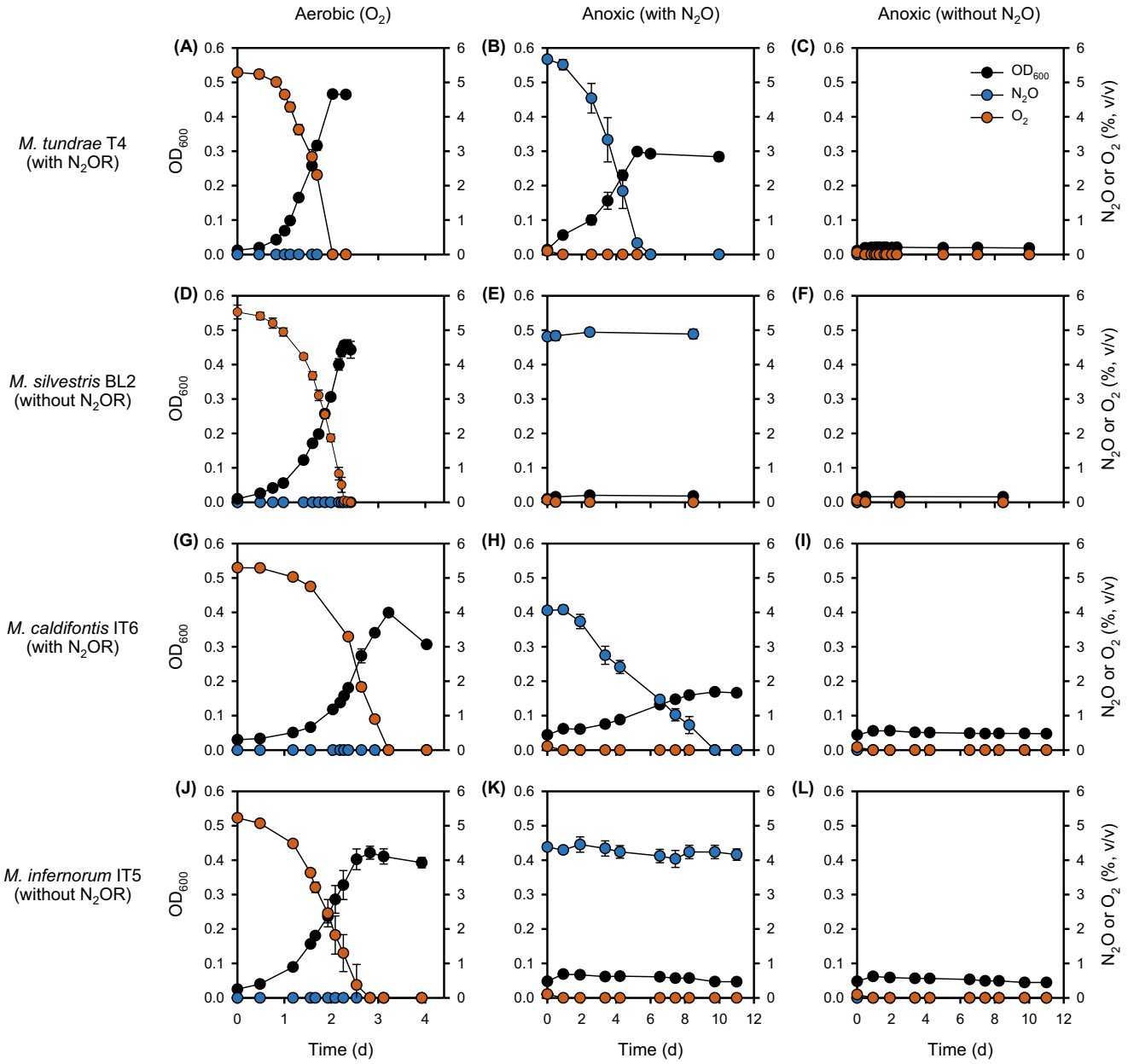

Fig. 2 | Aerobic and anaerobic growth of N_2OR-containing and N_2OR-lacking *Methylocella* and *Methylacidiphilum* strains on methanol. *Methylocella tundrae* T4, *Methylocella silvestris* BL2, *Methylacidiphilum caldifontis* IT6, and *Methylacidiphilum infernorum* IT5 cells were grown in LSM medium supplemented with 30 mM methanol as the electron donor and NH_4^+ as the N-source. Aerobic growth of the 4 strains with O_2 (**A**, **D**, **G**, **J**), anaerobic growth with N_2O (**B**, **E**, **H**, **K**), and anaerobic growth without N_2O (**C**, **F**, **I**, **L**) as the sole terminal electron acceptor were determined by optical density measurements at 600 nm, followed by measurements of O_2 and N_2O consumption in the headspaces of the culture bottles. Note that the trace O_2 present at the start of the incubation in the anaerobic cultures without N_2O did not contribute to obvious growth (**C**, **F**, **I**, **L**). All experiments were performed in triplicates. Data are presented as mean ± 1 standard deviation (SD), and the error bars are hidden when they are smaller than the width of the symbols. Source data are provided as Source Data file.

https://doi.org/10.1038/s41467-024-48161-z

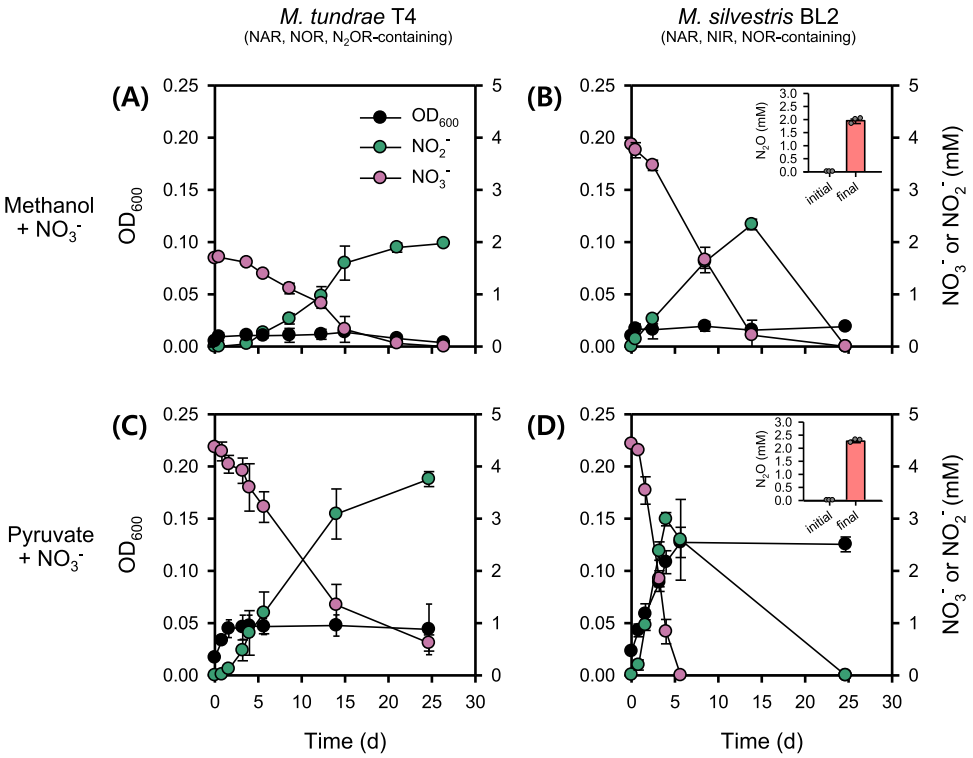

Fig. 3 | Anaerobic growth of *Methylocella* strains on methanol or pyruvate as the sole electron donor and NO_3^- as the terminal electron acceptor. *Methylocella tundrae* T4 and *Methylocella silvestris* BL2 cells were grown in LSM medium supplemented with 30 mM methanol and 2–4 mM NO_3^-. NH_4^+ (2 mM) was supplied as the N-source. Anaerobic growth of *Methylocella tundrae* T4 (**A**) and *Methylocella silvestris* BL2 (**B**) cells on methanol as the sole electron donor with NO_3^- as the sole electron acceptor. Anaerobic growth of *Methylocella tundrae* T4 (**C**) and *Methylocella silvestris* BL2 (**D**) cells on pyruvate as the sole electron donor with NO_3^- as the sole electron acceptor. N_2O produced from NO_3^- reduction by cells of *Methylocella silvestris* BL2 grown on methanol or pyruvate is shown as an inset plot within each figure. N_2O production was not observed in strain T4, hence inset plots for N_2O production were not displayed. Lower NO_3^- (ca. 2.0 mM) was used in the case of methanol (**A**) to avoid NO_2^- toxicity. Growth was determined by optical density measurements at 600 nm, followed by measurements of NO_3^- and NO_2^- concentrations. Data are presented as mean ± 1 SD of triplicate experiments, and the error bars are hidden when they are smaller than the width of the symbols. Source data are provided as Source Data file.

(FNA), a known inhibitor of microbial anabolic and catabolic processes[65]. In addition, chemodenitrification of NO_2^- (ref. 66) could result in an accumulation of NO in the cell environment, which is highly toxic to microbial life[67]. To further support the hypothesis of RNS toxicity, strain T4 was cultivated under N_2O-reducing conditions with methanol as the sole electron donor and supplied with NO_3^- instead of NH_4^+ as the N source in the medium (Supplementary Fig. 5). Consistent with the idea that NO_2^- accumulation results in growth arrest, the culture growth plateaued at approximately the same time NO_2^- accumulated (≥ 0.3 mM NO_2^-) (Supplementary Fig. 5A), whereas in control cultures containing NH_4^+ instead of NO_3^- as the N-source, NO_2^- accumulation was not observed, and the cells were able to reach higher cell densities (Supplementary Fig. 5B). Furthermore, the effect of NO_2^- stress induced in strain T4 was verified by adding varying NO_2^- concentrations (0, 0.01, 0.03, 0.1, 0.3, and 1 mM) to aerobic (Supplementary Fig. 6A) and anaerobic N_2O-respiring cultures (Supplementary Fig. 6B). Nitrite, particularly at concentrations higher than 0.3 mM at pH 5.5, induced stress in *Methylocella tundrae* T4, resulting in growth inhibition (Supplementary Fig. 6). These results are comparable to that of *Methylophaga nitratireducenticrescens* JAM1, a facultative methylotroph, which, when grown aerobically on methanol at pH 7.4, had a four-fold decrease in biomass in the presence of 0.36 mM NO_2^- and did not grow in the presence of 0.71 mM NO_2^- (ref. 68). Taken together, our data suggest that the failure of NO_3^-/NO_2^--reducing methanotrophs to grow on methanol may result from RNS toxicity. On the other hand, when N_2O is reduced to N_2 by N_2O-reducing methanotrophs, the creation of these RNS is avoided, which may explain the disparity in growth with N_2O as the terminal electron acceptor compared to NO_3^- and NO_2^-.

Toxicity of C1 metabolites in nitrate-reducing *Methylocella* species. Aside from the inhibitory effects of RNS, toxic intermediates from methanol metabolism might synergistically contribute to the inability of methanotrophs to grow when respiring NO_3^-/NO_2^-. Although formaldehyde is a key intermediate in the C1 metabolic pathway in many methylotrophs, it is highly toxic[69]. Therefore, in situations where biomass production is limited due to RNS toxicity, it is likely that formaldehyde further retards the growth of denitrifying methanotrophs. To investigate this mechanism, we grew *Methylocella* strains under NO_3^--reducing conditions using a C-C electron donor, pyruvate, which does not generate formaldehyde as a major metabolite (Figs. 3C, 3D). Eventually, nearly all the supplied NO_3^- was stoichiometrically converted to NO_2^- and N_2O in strains T4 and BL2, respectively. In contrast to the lack of growth on methanol, pyruvate supported the growth of both *Methylocella* strains under NO_3^--reducing conditions (Fig. 3C, D). Growth was more pronounced in strain BL2 than in strain T4 (Fig. 3C, D), possibly due to the presence of NIR and NOR in addition to NAR in strain BL2, which limited NO_2^- accumulation (Fig. 3D). Nonetheless, no further growth on pyruvate was observed in strain BL2 after day 5, despite reduction of the accumulated NO_2^- (~2.5 mM) to N_2O (Fig. 3D). It is worth noting that the accumulated NO_2^- concentration (Fig. 3D) is higher than the 0.3 mM concentration that inhibited *Methylocella tundrae* T4 (Supplementary Fig. 6) and may also be responsible for the lack of growth in strain BL2.

https://doi.org/10.1038/s41467-024-48161-z

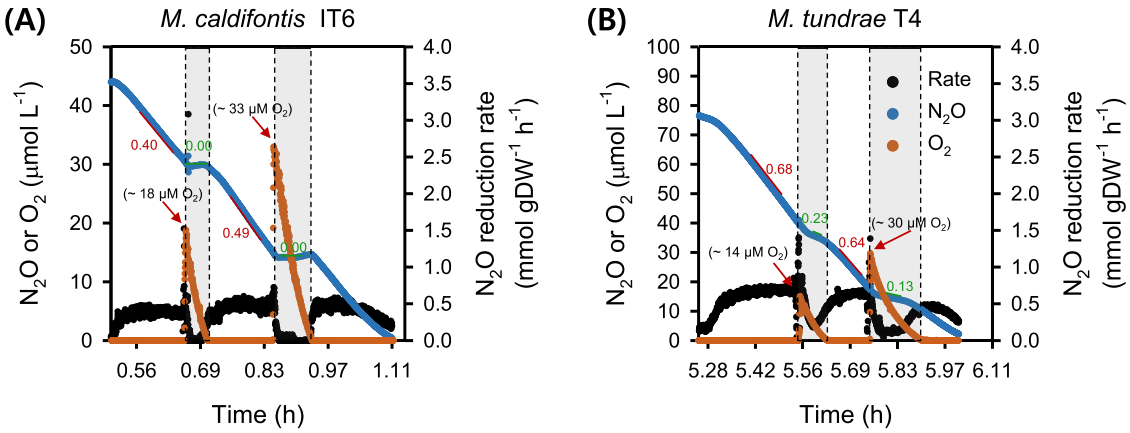

Fig. 4 | Microrespirometry-based N_2O and O_2 reduction during methanol oxidation by N_2OR-containing methanotrophs. N_2O and O_2 reduction by cells of *Methylacidiphilum caldifontis* IT6 (**A**) and *Methylocella tundrae* T4 (**B**) during methanol oxidation. Filled blue dots represent dissolved N_2O, filled orange dots represent dissolved O_2, and filled black dots represent N_2O reduction rates. Experiments were performed in a microrespirometry (MR) chamber fitted with O_2 and N_2O microsensors. The red arrows mark the addition of 14–33 μM O_2 into the MR chamber. The red- and green-marked numbers close to the red and green lines represent the N_2O reduction rates before and during O_2 reduction (gray-shaded area) in the MR chamber, respectively. Source data are provided as Source Data file.

Overall, these results demonstrate that in the tested *Methylocella* strains: (i) RNS have a major inhibitory effect on growth under denitrifying conditions; (ii) there are no growth benefits from methanol oxidation coupled to NO_3^- reduction, probably due to toxic C1 metabolic intermediates as well as RNS; and (iii) anaerobic growth is observed when NO_3^- reduction is coupled to the oxidation of pyruvate, a C-C electron donor; although the amount of growth is dependent on the completeness of the denitrification pathway and the accumulation of RNS. These propositions are supported by increased expression of genes involved in RNS and C1 metabolite detoxification under denitrifying conditions (see transcriptomic analysis below). Taken together, these results may explain why methanotrophs that couple methanol oxidation to NO_3^- or NO_2^- reduction show no clear signs of growth due to this process. Most methanotrophs can only utilize methane and its C1 derivatives as energy sources[70] and thus should not be able to grow under denitrifying conditions[21,22]. On the other hand, versatile facultative methanotrophs of the genus *Methylocella* are potentially able to grow in strictly anoxic habitats when alternative multi-carbon substrates are available. In terrestrial environments, various nitrogen oxides, originating from nitrification and denitrification processes, coexist and are spatiotemporally dynamic[71]. Thus, depending on the versatility of NO_2^- and NO reduction potential of methanotrophs as well as their coexistence with other NO_2^- and NO-reducing microorganisms, N_2O respiration can be supported or compromised (see Supplementary Figs 5, 6).

N_2O reduction coupled with CH_3OH or CH_4 oxidation

N_2O reduction kinetics. We investigated N_2O respiration kinetics using resting cells of anaerobic N_2O-respiring cultures ($CH_3OH + N_2O$) in a microrespirometry (MR) chamber. Harvested cells of strains *Methylacidiphilum caldifontis* IT6 and *Methylocella tundrae* T4 were dispensed into a closed 10-mL MR chamber outfitted with O_2 and N_2O-detecting microsensors, supplied with CH_3OH (2 mM) and N_2O as a sole electron donor and acceptor, respectively, and incubated anoxically. The N_2O respiration kinetics followed Michaelis-Menten kinetics (Supplementary Fig. 7, Supplementary Note 2). The cells of strains T4 and IT6 grown at anoxic $CH_3OH + N_2O$ conditions reduced N_2O at a maximum rate of 1.122 ± 0.005 mmol $N_2O{\cdot}h^{-1}{\cdot}g\ DW^{-1}$ (Supplementary Fig. 7A) and 0.414 ± 0.003 mmol $N_2O{\cdot}h^{-1}{\cdot}g\ DW^{-1}$ (Supplementary Fig. 7B), respectively. The molar ratios of CH_3OH to O_2 and CH_3OH to N_2O consumed were approximately 1:1.0 (± 0.05; $n = 3$) and 1:2.04 (± 0.17; $n = 3$), respectively, which coincide with the theoretical values obtained from Eqs. 3 and 4.

$$CH_3OH + O_2 \rightarrow 0.5CO_2 + 1.5H_2O + 0.5CH_2O(\text{biomass}) \quad (3)$$

$$CH_3OH + 2N_2O \rightarrow 0.5CO_2 + 1.5H_2O + 2N_2 + 0.5CH_2O(\text{biomass}) \quad (4)$$

Sensitivity of N_2OR to O_2. While O_2 is well known to impair N_2OR activity[72], some bacterial strains have been reported to reduce N_2O in the presence of O_2 (refs. 73,74). We therefore tested the capacity of strains IT6 and T4 to reduce N_2O in the presence of O_2 by using resting cells of anoxic $CH_3OH + N_2O$ cultures. After spiking O_2 to strain IT6 cells respiring N_2O in the anoxic MR chamber, N_2O-respiration ceased: dropping from the maximum (0.4–0.5 mmol $N_2O{\cdot}h^{-1}{\cdot}g\ DW^{-1}$) to zero (Fig. 4A, Table 1). N_2O reduction activity only started when the dissolved O_2 concentration was below ca. 3 μM, suggesting the N_2O reduction activity of this strain is highly sensitive to O_2. In contrast, when O_2 (~ 14 and 30 μM) was added to N_2O-respiring cells of strain T4, simultaneous reduction of N_2O and O_2 was observed (Fig. 4B). However, the N_2O respiration rates dropped to 0.24 and 0.13 mmol $N_2O{\cdot}h^{-1}{\cdot}g\ DW^{-1}$ after spiking ~14 and 30 μM O_2, respectively, which were approximately 34 and 20% of the maximum rate before O_2 introduction (0.64–0.68 mmol $N_2O{\cdot}h^{-1}{\cdot}g\ DW^{-1}$). These results suggest that in contrast to strain IT6, N_2O reduction in strain T4 is not highly impaired by O_2. N_2OR activity fully recovered in both strains after O_2 was depleted. Because the N_2OR of strain IT6 was found to be highly sensitive to O_2, further characterization of methanotroph N_2OR activity in response to O_2 exposure was limited to strain T4.

Considering these results, we set out to see if cells of strain T4 could continue N_2O respiration while using O_2 for CH_4 oxidation in the MR chamber. The cells used for this experiment were cultured in suboxic conditions with starting gas mixing ratios (v/v) of 1% O_2, 5% N_2O, and 20% CH_4 (i.e., $CH_4 + O_2 + N_2O$ condition). Similar to the anoxic $CH_3OH + N_2O$-adapted cells described above, the suboxic $CH_4 + O_2 + N_2O$-adapted cells co-respired O_2 and N_2O after injecting CH_4 (~406 μM) into a 5-mL MR chamber containing O_2 (~30 μM) and N_2O (~480 μM) (Fig. 5A). Interestingly, the maximum N_2O respiration rates during each O_2 spike were 1.4 to 2 times higher (1.58–2.47 mmol $N_2O{\cdot}h^{-1}{\cdot}g\ DW^{-1}$) in the suboxic $CH_4 + O_2 + N_2O$-adapted cells (Fig. 5B, Table 1) than in the anoxic $CH_3OH + N_2O$-adapted cells (1.12 ± 0.01 mmol $N_2O{\cdot}h^{-1}{\cdot}g\ DW^{-1}$) (Table 1, Supplementary Fig. 7B), suggesting that the cells can modulate the rates of N_2O reduction in response to O_2 availability.

https://doi.org/10.1038/s41467-024-48161-z

Table 1 | Microrespirometry-based substrate-specific N_2O- or O_2-reduction rate by *Methylocella tundrae* T4 cells grown under anoxic and suboxic growth conditions

Condition	Rate (mmol·h^{-1}·g DW^{-1})
Maximum respiration rates of anoxic $CH_3OH + N_2O$-respiring cells	
N_2O respiration (at 0 μM O_2; electron donor CH_3OH; at the first 4 spikes of N_2O)	1.12 ± 0.01
N_2O respiration (at 0–5 μM O_2; electron donor CH_3OH; at the 5th spikes of N_2O)	0.64–0.68
N_2O respiration (at O_2 > 5 μM; electron donor CH_3OH)	0.13–0.24
O_2 respiration (at O_2 > 5 μM; electron donor CH_3OH)	1.02–1.07
Maximum respiration rates of suboxic $CH_4 + N_2O + O_2$-respiring cells	
N_2O respiration (at 25–60 μM O_2; electron donor = CH_4)	1.58–2.47
N_2O respiration (at 5–170 μM O_2; electron donor = CH_4)	1.32 ± 0.25
O_2 respiration (at 25–60 μM O_2; electron donor = CH_4)	0.98–2.37
O_2 respiration (at 5–170 μM O_2; electron donor = CH_4)	0.95 ± 0.09

These values were obtained from respiration activities with cells that had CH_3OH or CH_4 as the sole electron donor.

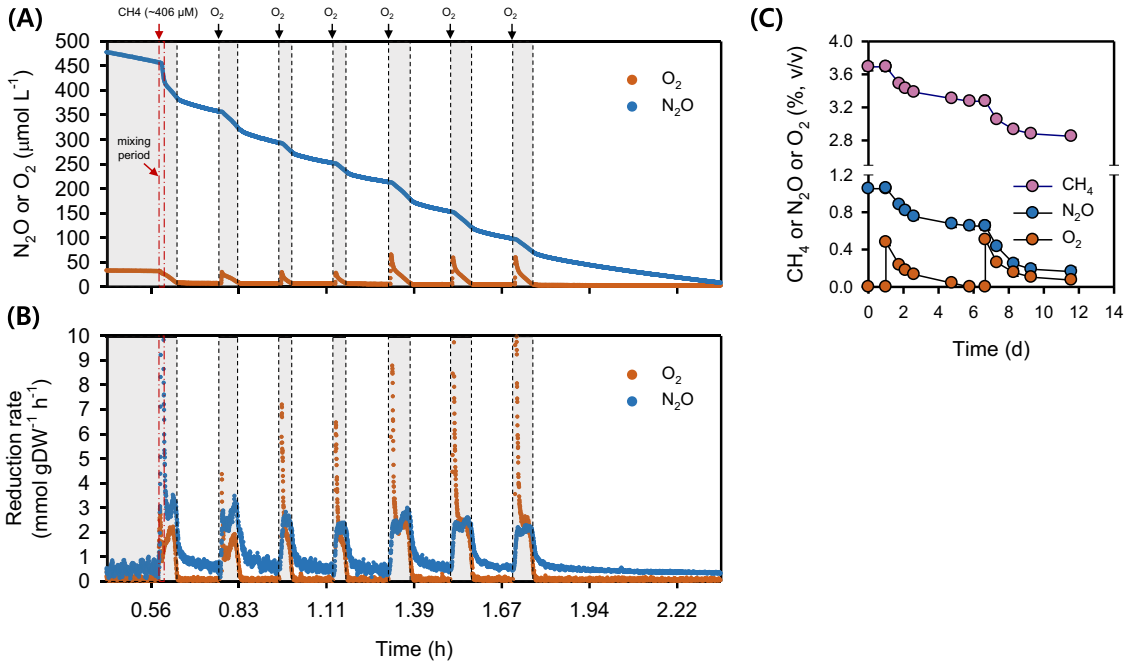

Fig. 5 | Simultaneous N_2O and O_2 reduction by *Methylocella tundrae* T4 cells during CH_4 oxidation in microrespirometry (MR) and growth experiments. **A** MR experiment showing the simultaneous reduction of N_2O and O_2 by *Methylocella tundrae* T4 cells during CH_4 oxidation. **B** N_2O and O_2 reduction rates by cells of strain T4 during CH_4 oxidation calculated from (**A**). The filled orange and blue dots in the upper (**A**) represent the concentrations of dissolved O_2 and N_2O, respectively. The filled orange and blue dots in the bottom (**B**) represent the rates of O_2 and N_2O reduction, respectively. Experiments were performed in a MR chamber fitted with O_2 and N_2O microsensors. The red arrow marks the addition of CH_4 (~406 μM) into the MR chamber. The black arrow marks the addition of ~26 μM or ~60 μM O_2 into the MR chamber. The gray-shaded area represents points where N_2O and O_2 are reduced simultaneously. **C** Growth experiment showing *Methylocella tundrae* T4 cells reducing N_2O and O_2 simultaneously during CH_4 oxidation. The culture was grown in 2-liter sealed bottles (triplicates) containing 60 mL of LSM medium with 2 mM NH_4^+ as the N-source. The headspace of the bottles was composed of CH_4 (5%, v/v), O_2 (0.5%, v/v), N_2O (1.4%, v/v), and CO_2 (5%, v/v) and supplemented with additional O_2 (~0.5%, v/v) before its depletion. The incubation period shown in (**C**) is after the initial 20-day incubation period. After the depletion of O_2, additional O_2 was spiked to observe the simultaneous reduction of O_2 and N_2O during CH_4 oxidation. Data are presented as the mean ± 1 SD of a triplicate experiment, and the error bars are hidden when they are smaller than the width of the symbols. Source data are provided as Source Data file.

Accordingly, the maximum rates of N_2O reduction (1.58–2.47 mmol N_2O·h^{-1}·g DW^{-1}) and O_2 reduction (0.98–2.37 mmol O_2·h^{-1}·g DW^{-1}) by the suboxic $CH_4 + O_2 + N_2O$-adapted cells were comparable (Fig. 5B, Table 1). As the O_2 concentration and reduction rate decreased, the N_2O reduction rate also decreased (Fig. 5A, B), revealing that activation of CH_4 by O_2 is required for stimulating N_2O respiration by $CH_4 + O_2 + N_2O$-adapted cells. Based on these results, we conclude that, under suboxic conditions, both aerobic CH_4 oxidation and N_2O reduction were operating in concert: O_2 was needed for the monooxygenase, but the N_2OR remained active and was able to accept electrons released downstream in the C1 oxidation pathway. This adds to the evidence that aerobic N_2O respiration occurs in strain T4 and is linked to aerobic CH_4 oxidation.

Finally, we estimated the O_2 concentration range at which the suboxic $CH_4 + O_2 + N_2O$-adapted cells of strain T4 show N_2O-reducing activity. At a O_2 concentration of 170 μM, O_2 and N_2O were reduced simultaneously (Supplementary Fig. 8A, B). The maximum N_2O reduction rate (Table 1) was nearly constant (1.32 ± 0.25 mmol

Table 2 | The effect of N_2O addition on CH_4-oxidizing cultures of *Methylocella tundrae* T4 growing in suboxic conditions

Culture condition	CH_4 oxidized (mmol·L^{-1})	O_2 reduced (mmol·L^{-1})	N_2O reduced (mmol·L^{-1})	Increase in OD_{600}
$CH_4 + O_2$	9.74 ± 0.39	14.93 ± 0.43	NA	0.114 ± 0.006
$CH_4 + O_2 + N_2O$	12.19 ± 0.24	13.96 ± 0.41	10.15 ± 0.35	0.143 ± 0.002

The experiment was performed in 2-liter sealed bottles (replicates) with 60 mL of LSM medium in an O_2-limiting suboxic headspace with and without N_2O (0.5% O_2, 5% CH_4, 5% CO_2, and 0 or 1% N_2O). Following the observation of N_2O reduction in bottles containing N_2O, the headspace O_2 and N_2O mixing ratios in the bottles were increased to approximately 1% and 2% (v/v), respectively. The reduction of N_2O by the cultures increased CH_4 oxidation and biomass compared to cultures containing only O_2. Data are presented as mean ± 1 SD ($n = 3$). NA not available.

$N_2O \cdot h^{-1} \cdot g\ DW^{-1}$) across the O_2 concentration range of 5–170 μM (Supplementary Fig. 8B, C) and was about 1.4 times higher than the maximum O_2 reduction rates (0.95 ± 0.09 mmol $O_2 \cdot h^{-1} \cdot g\ DW^{-1}$). This means that even when exposed to high levels of O_2, the N_2OR in the suboxic $CH_4 + O_2 + N_2O$-adapted cells remained functional and could reduce N_2O at high rates. Other bacterial strains' N_2OR activities have been reported at O_2 concentrations between 100 and 260 μM (refs. 73,74), indicating that their N_2OR activity is similarly O_2-tolerant[73] as that of strain T4. According to the findings of Wang and colleagues[73], N_2O reducers with an O_2 tolerant N_2OR maintain low internal O_2 concentrations in their cells by rapidly consuming O_2, allowing the N_2OR to remain active. However, it remains unclear if *Methylocella tundrae* T4 employs a similar strategy to maintain an O_2-tolerant N_2OR.

Improved methanotrophic growth of *Methylocella tundrae* in the presence of N_2O. Based on the MR experiments showing the simultaneous reduction of O_2 and N_2O by CH_4-fed cells of strain T4, alongside the clear N_2O-dependent anaerobic growth, we hypothesized that strain T4 growth can be enhanced when it oxidizes CH_4 by simultaneously reducing O_2 and N_2O under suboxic conditions. Using fed-batch growth experiments, we verified that strain T4 grows by CH_4 oxidation coupled with co-respiration of N_2O and O_2 (Fig. 5C, Table 2), strongly supporting the MR results above. Cells grown under the suboxic $CH_4 + O_2 + N_2O$ condition consumed roughly the same amount of O_2 and N_2O (Fig. 5C, Table 2), and these values were comparable to what $CH_4 + O_2 + N_2O$-grown cells consumed in the MR experiments (see Fig. 5A). Consequently, our results demonstrate that in an O_2-limited environment, the cells can benefit energetically by directing more O_2 to the monooxygenase step of CH_4 oxidation, and simultaneously running a hybrid ($O_2 + N_2O$) electron transport system as shown in Table 2 and Fig. 5C.

The data showed unequivocally that the total electron equivalents released during CH_4 oxidation to CO_2 could account for the total electron acceptor ($O_2 + N_2O$) reduced. Based on a CH_4 to O_2 ratio of 1:1.57 (ref. 75), the total amount of O_2 reduced (13.96 mmol·L^{-1}) by the suboxic $CH_4 + O_2 + N_2O$ cultures could theoretically only account for 8.89 mmol·L^{-1} oxidized CH_4. However, a larger total of 12.19 mmol·L^{-1} CH_4 was oxidized by this culture (Table 2), and the excess 3.29 mmol·L^{-1} must have required an additional electron acceptor (i.e., N_2O). Consistently, about 10.15 mmol·L^{-1} N_2O was reduced by the suboxic $CH_4 + O_2 + N_2O$ cells, equivalent to 5.08 mmol·L^{-1} O_2, since half as many electrons are consumed per mol during N_2O reduction to N_2 compared to O_2 reduction to H_2O. By running the N_2O respiration system, the cells lower their O_2-demand for respiration by the aerobic terminal oxidase and maximize O_2 use by the methane monooxygenase[76]. Due to having more CH_4 oxidized per O_2 reduced (~37%) when N_2O is present, higher cell densities (OD_{600}) per O_2 reduced (~34%) were reached in the suboxic $CH_4 + N_2O + O_2$ cultures than in the O_2-replete $CH_4 + O_2$ cultures (Table 2), further demonstrating the beneficial contribution of N_2O reduction to growth on CH_4 at suboxic conditions.

Transcriptomics

The overall regulation of key genes involved in denitrification and methane oxidation is depicted in Fig. 6 as well as in the supplementary material (Supplementary Figs. 9, 10, 11, Supplementary Datasets 5, 6, 7). Differences in expression were considered significant if the Log_2FC was higher than [0.85] or lower than [-1.0] with an adjusted $p \leq 0.05$.

N_2OR (O_2 replete vs. anoxic conditions). The transcript levels of the N_2OR-encoding genes (T4_03941–7), *nosRZDFYLX*, were 2- to 4.7-fold higher in strain T4 cells respiring N_2O in the anoxic $CH_3OH + N_2O$ conditions compared to strain T4 cells respiring O_2 in the O_2-replete $CH_3OH + O_2$ conditions (Fig. 6 Supplementary Datasets 5, 6). Cells of strain IT6 respiring N_2O in the anoxic $CH_3OH + N_2O$ conditions showed transcriptional upregulation (1.9–6.7-fold) of four *nos* genes (*nosC1BZC2*) under anoxic conditions (Supplementary Fig. 10, Supplementary Dataset 7). Other *nos* operon genes (*nosYFDL*; IT6_00904–11) were expressed constitutively under both the anoxic $CH_3OH + N_2O$ and O_2-replete $CH_3OH + O_2$ conditions. The NosC1 and NosC2 proteins of *Wolinella succinogenes* were predicted to facilitate electron transfer from menaquinol to the periplasmic NosZ during the reduction of N_2O to N_2 (ref. 47) and are likely to play a similar role in strain IT6. Although the exact function of NosB has yet to be elucidated, Hein and colleagues[77] used a non-polar *nosB* deletion mutant of *Wolinella succinogenes* to show that it is necessary for N_2O respiration. Overall, increased expression of N_2OR-encoding genes in *Methylocella tundrae* T4 and *Methylacidiphilum caldifontis* IT6 cells during anaerobic growth indicates that the N_2OR is functional in these methanotrophs and supports their ability to respire and grow using N_2O as a terminal electron acceptor.

N_2OR (O_2 replete vs. suboxic conditions). Transcript levels of N_2OR-encoding genes were 2–10.7-fold higher in strain T4 cells grown under suboxic $CH_4 + O_2 + N_2O$ conditions than in cells grown under O_2-replete $CH_4 + O_2$ conditions (Supplementary Fig. 9, Supplementary Datasets 5, 6). This finding is consistent with the N_2O respiration activity and growth of strain T4 under suboxic $CH_4 + O_2 + N_2O$ conditions (Fig. 5), in which the cells can efficiently oxidize more CH_4 (see Table 2), most likely because the use of N_2O for cellular respiration allows them to devote more O_2 to CH_4 oxygenation.

Methanol dehydrogenase (O_2 replete vs. anoxic conditions). In methanotrophs, methanol oxidation occurs in the periplasmic space by PQQ (pyrroloquinoline quinone)-dependent methanol dehydrogenase (MDH). Seven PQQ-dependent alcohol dehydrogenases (ADHs)[78] are encoded in the genome of strain T4 (Supplementary Dataset 5). Five are type I ADHs (quinoproteins), which include one calcium-dependent MDH (MxaF-type MDH), and four lanthanide-dependent MDHs (XoxF-type MDH), divided into clades 1 (XoxF1), 3 (XoxF3), and 5 (XoxF5; 2 copies) (Supplementary Fig. 12). The other two are type II ADHs (quinohemoproteins). In addition to the PQQ-dependent ADH, *Methylocella tundrae* T4 and *Methylacidiphilum caldifontis* IT6 genomes contain genes encoding cytosolic Zn^{2+}-dependent ADH, which are part of a large family of enzymes that oxidize alcohols to aldehydes or ketones and reduce $NAD(P)^+$ or a similar cofactor[79] (Supplementary Datasets 5, 6).

Among the four XoxF-type MDHs encoded in the genome of strain T4, genes in a *xoxFGJ* operon (T4_03519–21), which include a gene encoding a XoxF5 enzyme, were found to be constitutively transcribed at high levels in cells grown under both O_2-replete $CH_3OH + O_2$ and

https://doi.org/10.1038/s41467-024-48161-z

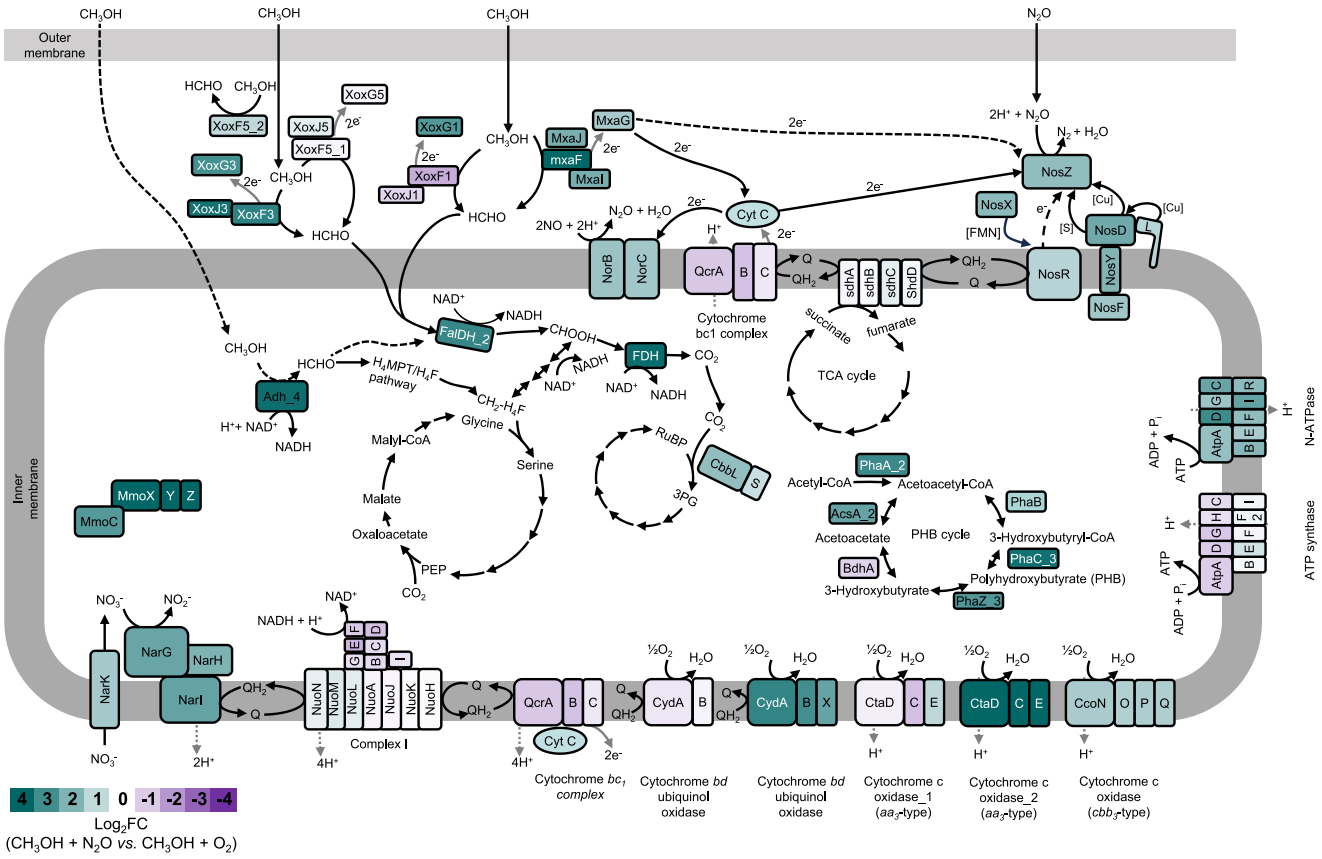

Fig. 6 | Metabolic reconstruction and transcriptional response of *Methylocella tundrae* T4 cells to O_2-replete ($CH_3OH + O_2$) and anoxic ($CH_3OH + N_2O$) methanol-oxidizing growth conditions. The genes used to reconstruct the metabolic pathway are listed in Table S5. The gene products are shaded according to the relative fold change (Log_2FC) in gene expression between cells grown under anoxic ($CH_3OH + N_2O$) and O_2-replete ($CH_3OH + O_2$) conditions. Genes up-regulated in $CH_3OH + N_2O$-grown cells are shown in teal green, while those up-regulated in $CH_3OH + O_2$-grown cells are shown in purple. Note that proteins are not drawn to scale. Methanol oxidation: Methanol is oxidized to formaldehyde in the periplasmic space by the PQQ-dependent methanol dehydrogenase (Xox- and Mxa-type), T4_03519–21, T4_00353–5, and T4_01862–76. The $NAD(P)^+$-dependent alcohol dehydrogenase (T4_03199) may also be involved in methanol oxidation to formaldehyde in the cytoplasmic space during anaerobic growth on methanol. Formaldehyde oxidation to formate then proceeds via the tetrahydromethanopterin (H_4MPT) pathway, and C1 incorporation into the serine cycle is mediated by the tetrahydrofolate (H_4F) carbon assimilation pathway. The Calvin-Benson-Bassham pathway is also a possible route for CO_2 fixation. Nitrous oxide reduction: N_2O is reduced to N_2 through the activity of nitrous oxide reductase in the periplasmic space. Electron transfer to NosZ occurs via cytochrome c from the cytochrome bc1 (Qcr) complex[136,137]. Electron transfer to the NosZ may also involve direct interaction with methanol dehydrogenase C-type cytochrome (XoxG, MxaG). The NosR protein may be involved in the transfer of electrons to NosZ (refs. 136,137).

anoxic $CH_3OH + N_2O$ conditions (Fig. 6, Supplementary Datasets 5, 6). Thus, the *xoxF5* gene likely encodes the predominant MDH used by strain T4 in both O_2-respiring and N_2O-respiring cells. The other singleton *xoxF5* gene (T4_03691) and a *xoxF3* gene found in a separate *xoxFGJ* cluster (T4_00353–5) were also significantly upregulated in cells grown under anoxic $CH_3OH + N_2O$ conditions in comparison to cells grown under O_2-replete $CH_3OH + O_2$ conditions (Fig. 6, Supplementary Datasets 5, 6). Furthermore, we observed a significant upregulation (2- to 22-fold) of the genes encoding MxaFI-type MDH (T4_01872–6) in the anoxic $CH_3OH + N_2O$-grown cells (Fig. 6, Supplementary Datasets 5, 6). Thus, our results indicate the use of various MDHs by strain T4 during anaerobic growth. In strain IT6 a *xoxF* gene encoding a XoxF2-type MDH is present as part of the *xoxGJF* operon (IT6_00336–8) (Supplementary Dataset 7) and the expression of the *xoxF2* gene was 2-fold upregulated in the N_2O-respiring cells (Supplementary Fig. 10, Supplementary Dataset 7).

A cytosolic Zn^{2+}-dependent ADH bound to $NAD(P)^+$ is known to perform the oxidation of methanol in Gram-positive methylotrophs[80]. A Zn^{2+}-dependent ADH (T4_03199) of strain T4 was significantly upregulated (13.8-fold) in the anoxic $CH_3OH + N_2O$-grown cells compared to the O_2-replete $CH_3OH + O_2$-grown cells (Fig. 6, Supplementary Datasets 5, 6). Strain IT6 genome also contained three copies of genes encoding enzymes annotated as Zn^{2+}-dependent ADH (Supplementary Dataset 7). The expression of two of these genes (IT6_01501 and IT6_01931) were 3.9-fold and 2.5-fold upregulated in N_2O-respiring cells compared to cells respiring O_2 (Supplementary Fig. 10, Supplementary Dataset 7). Even though PQQ-dependent MDHs have a high-affinity for and activity with methanol as a substrate, their use in strictly anoxic conditions will be limited because PQQ biosynthesis requires molecular oxygen[81]. Thus, PQQ-dependent MDHs are suggested to be functional at completely anoxic conditions only when PQQ is carried over from an aerobic growth stage or provided externally[82]. On the other hand, Zn^{2+}-dependent MDHs have the advantage of utilizing a ubiquitous cofactor, $NAD(P)^+$, and can be functional during anaerobic growth[83]. This finding raises the possibility that strains T4 and IT6 can employ alternative ADHs such as the Zn^{2+}-dependent ADH to facilitate methanol oxidation in strict anoxia. Some genes required for the subsequent steps of C1 metabolism, i.e., formaldehyde and formate dehydrogenases, were also upregulated in strain T4 (but not IT6) growing anaerobically. These are depicted in Fig. 6 and supplementary materials (Supplementary Fig. 9, Supplementary Dataset 5).

Methanol dehydrogenase (O_2 replete vs. suboxic conditions). Furthermore, we also examined expression levels of genes encoding MDHs in strain T4 cells grown under suboxic $CH_4 + O_2 + N_2O$ conditions (Supplementary Fig. 9, Supplementary Datasets 5, 6). Genes in the cluster T4_01862–76, which encodes the calcium-dependent MDH (MxaF-type MDH), had the highest transcript expression among all MDH-encoding genes in CH_4-oxidizing cells grown under suboxic $CH_4 + O_2 + N_2O$ conditions. When compared to O_2-replete $CH_4 + O_2$ conditions, the expression of genes within this cluster was 1.8- to 371.5-fold upregulated (Supplementary Fig. 9, Supplementary Datasets 5, 6). This is unexpected since genes encoding the Mxa-type MDH are typically downregulated in the presence of lanthanides[84]; which we also included (2 μM each of cerium and lanthanum) in the growth medium. Their apparent upregulation (even when lanthanides are present) suggests that this enzyme might play an important role in CH_4 metabolism in the presence of N_2O and suboxic conditions. As observed above, genes in the *xoxFGJ* operon (T4_03519–21) were also highly expressed at the suboxic conditions (Supplementary Fig. 9, Supplementary Datasets 5, 6), suggesting that this key MDH is used by strain T4 in all three conditions. Genes in the cluster T4_01892–4 including the gene encoding the XoxF1 MDH were also significantly upregulated (18- to -35-fold) in the suboxic $CH_4 + O_2 + N_2O$-grown cells compared to the O_2-replete $CH_4 + O_2$-grown cells. The operon T4_02097–8, which encodes a cytochrome *c*550 (T4_02097) and a type II ADH (T4_02098), exhibited 6-fold and 30.6-fold upregulation, respectively, in cells grown under suboxic $CH_4 + O_2 + N_2O$ conditions as opposed to cells grown under O_2-replete $CH_4 + O_2$ conditions. In addition, two Zn^{2+}-dependent ADHs (T4_03097 and T4_03199) were significantly upregulated (3.5-fold and 46-fold, respectively) in strain T4 cells grown under suboxic $CH_4 + O_2 + N_2O$ conditions compared to cells grown under O_2-replete $CH_4 + O_2$ conditions. Overall, it appears that cells oxidizing methanol under anoxia ($CH_3OH + N_2O$-grown cells) or those oxidizing methane under suboxia ($CH_4 + O_2 + N_2O$-grown cells) use a distinct set of MDHs from those they use during O_2 respiration.

Methane monooxygenase. The genomes of *Methylocella tundrae* T4 and *Methylacidiphilum caldifontis* IT6 contain genes that encode sMMO and pMMO, respectively. In the suboxic $CH_4 + O_2 + N_2O$ conditions, all the genes (*mmoXYBZDCRG*) in the gene cluster T4_01946–54 displayed a high degree of transcriptional upregulation (18.7–96-fold) compared to O_2-replete CH_4 conditions (Supplementary Fig. 9, Supplementary Datasets 5, 6). In a previous study[85], *Methylosinus trichosporium* OB3b sMMO activity and protein expression were found to be significantly elevated under hypoxic conditions (24 μM) compared to higher O_2 conditions (188 μM). Furthermore, *Methylosinus trichosporium* OB3b sMMO's catalytic activity in the degradation of dichloroethane was enhanced at low O_2 levels and impaired at elevated O_2 levels[86]. Thus, in methanotrophs, upregulation of methane monooxygenase genes under O_2 limiting conditions might be a strategy to produce more methane monooxygenase. This will lead to increased methane oxidation and thus provide stronger competition for the limited O_2 with the terminal oxidase. Aside from the methane monooxygenase genes, group II and III truncated hemoglobin encoding genes were upregulated in *Methylocella tundrae* T4 (T4_02445, T4_02637, and T4_00400; 4- to 12-fold) and *Methylacidiphilum caldifontis* IT6 (IT6_00149; 3-fold) cells in response to suboxia or anoxia (Supplementary Datasets 5, 6). These truncated hemoglobins are thought to transport O_2 to the methane monooxygenase[22]. Compared to methane, methanol resulted in lower transcript levels of sMMO genes in *Methylocella tundrae* T4 (Supplementary Fig. 11, Supplementary Dataset 5), with much lower levels in the O_2 replete $CH_3OH + O_2$ conditions compared to the anoxic $CH_3OH + N_2O$ conditions (Fig. 6, Supplementary Datasets 5, 6). Transcriptional repression of sMMO genes by growth substrates other than methane has been observed in *Methylocella silvestris* BL2 (refs. 87,88). The expression of genes encoding denitrification enzymes, their transcriptional regulators, and terminal oxidase is described in Supplementary Note 3.

Ecological relevance

Our findings revealed that certain methanotrophic strains, particularly those from the genera *Methylocella* and *Methylocystis*, which are commonly found in acidic and neutral terrestrial environments based on ecological meta-data from the BacDive database[89,90], have the ability to reduce N_2O. Wetlands, such as acidic peatlands and paddy fields, are significant contributors to the release of CH_4 and N_2O (refs. 27,91,92). Although active N_2O consumption has been observed in acidic wetlands[93], little is known about the microbial mechanisms that drive these processes. In a recent study[27] wherein active N_2O consumption was observed in peatlands (pH 6.4–3.7) located in Central and South America, *Methylocystis* species accounted for over 20% of the N_2O-reducing microbial community based on *nosZ* gene amplicon sequence variants. This implies that N_2OR-containing methanotrophs might make significant contributions to N_2O reduction in these environments. The current prevailing perception of N_2OR containing methanotrophs as a phylogenetically narrow group with limited ecological impact might be heavily biased by the scarcity of cultured methanotrophs with such metabolic capabilities. Thus, additional in situ and ecogenomic-based investigations are needed to more precisely quantify the contribution of known methanotrophs to N_2O reduction as well as to uncover other novel N_2O-reducing methanotrophs, such as those belonging to the *Gemmatimonadota* phylum[50].

Short-term or seasonal water table fluctuations caused by either natural or anthropogenic desiccation influence the transition zone from oxic to anoxic conditions in wetlands[94–96]. In the deeper, water-filled anoxic layer of wetlands[97], and even in oxygenated wetland soils[98], methanogens produce CH_4. N_2O can be produced from denitrification processes, especially by incomplete denitrifiers which are frequently abundant in environments[30–32]. Nitrifiers also produce a significant amount of N_2O as a byproduct of ammonia oxidation in the suboxic layers[99]. Furthermore, NO_2^- produced from nitrogen cycling processes can be abiotically reduced to N_2O through chemodenitrification due to the stability of Fe^{2+} in acidic peat soils. At the oxic-anoxic interface, where CH_4 and O_2 gradients overlap, N_2O-respiring methanotrophs will have simultaneous access to both CH_4 and N_2O. Although the CH_4-O_2 counter gradient is dynamic and O_2-respiring organisms can rapidly deplete the limited O_2, these N_2O-respiring methanotrophs can use a growth strategy that involves respiring both N_2O and O_2 and coupling it to CH_4 oxidation. This unique lifestyle, combined with the potential ability to respire N_2O solely with non-methane substrates such as C1, C-C compounds[51,100] as well as H_2 (refs. 52,100), can confer a selective growth advantage, facilitate their niche expansion to suboxic and anoxic zones, and make them resilient in such environments.

In conclusion, we revealed that sMMO- and pMMO-containing acidophilic methanotrophs of the genera *Methylocella* and *Methylacidiphilum* can grow anoxically by respiring N_2O using clade I and II NosZ, respectively. N_2O reduction was detected at an extremely acidic pH of 2.0, which is by far the lowest pH reported for this process[27,92]. Further, N_2O reduction can improve the growth yields of these bacteria under O_2-limiting conditions and provide a competitive advantage. This study significantly expands our perception of the potential ecological niches of aerobic methanotrophs. In addition to mitigating CH_4 and CO_2 emissions, aerobic methanotrophs potentially play a role in reducing the emission of the climate-active and ozone-depleting gas N_2O, particularly in low pH environments.

Methods

Bacterial strains and growth conditions

The methanotrophic bacterial strains used for the experiments include *Methylacidiphilum caldifontis* IT6, *Methylacidiphilum infernorum* IT5,

Methylocella tundrae T4 (=KCTC 52858 T), *Methylocella silvestris* BL2 (=KCTC 52857 T), *Methylocystis* sp. SC2, and three in-house *Methylocystis echinoides*-like isolates (strains IM2, IM3, and IM4). The *Methylacidiphilum* strains are also in-house strains isolated previously from a mud-water mixture taken from Pisciarelli hot spring in Pozzuoli, Italy[44]. The *Methylocella* strains were obtained from the Korean Collection for Type Cultures (KCTC). Growth of the bacterial strains was performed using a low salt mineral (LSM) medium. The medium contained 0.4 mM $MgSO_4 \cdot 7H_2O$, 0.2 mM K_2SO_4, and 0.1 mM $CaCl_2 \cdot 2H_2O$ and was supplemented with filter-sterilized solutions of 2 mM $(NH_4)_2SO_4$, 0.1 mM KH_2PO_4, 1 μM $CeCl_3$, 1 μM $LaCl_3$, 1 mL (1×) vitamin, and 1 mL (1×) trace element solutions[101] per liter. The pH of the medium was adjusted to pH 2.0 with concentrated sulfuric acid (filter-sterilized) for the *Methylacidiphilum* strains and to pH 5.5 with 20 mM 2-morpholinoethanesulfonic acid (filter-sterilized) for the *Methylocella* strains. The cultures were incubated at 52 °C for *Methylacidiphilum* strains (IT5 and IT6) and 28 °C for *Methylocella* strains (T4 and BL2) with shaking at 160 rpm. Unless stated otherwise, ammonium sulfate, $(NH_4)_2SO_4$, was used as the nitrogen source.

Enrichment and isolation of *Methylocystis* strains

The N_2OR-containing *Methylocystis* strains were isolated from an acidic forest soil in Chungcheongbuk-do, South Korea (36°55'31" N 127°54'86" E). The soil sample preparation and initial enrichment of the methanotrophs[102], as well as the isolation of methanotrophic strains through repeated serial dilution of the enrichment cultures[103], have all been described previously. Briefly, the most diluted culture exhibiting methane oxidation was serially diluted and filtered through 0.2-μm Track-Etch membrane polycarbonate filters (Whatman). The filters were placed on LSM medium (pH 5.5) in Petri dishes and incubated at 30 °C in airtight containers containing CH_4 (10%, v/v) and CO_2 (5%, v/v). Colonies that appeared on the filters after 3 weeks of incubation were transferred to fresh LSM medium in 160-mL serum vials with the same gas composition. Three individual methanotrophic isolates were identified by sequencing the 16 S rRNA gene with the 27 F/1492 R primer set[104]. The purity of the isolates was confirmed by seeding aliquots of the CH_4-grown cultures into the LSM medium with 0.05% (w/v) yeast extract, tryptic soy broth, and Luria-Bertani broth without CH_4 and incubating at 30 °C. Three methanotrophic isolates, IM2, IM3, and IM4, shared 99.46% 16 S ribosomal RNA (rRNA) gene-sequence identity with the alphaproteobacterial methanotroph *Methylocystis echinoides* LMG27198. The three strains share average nucleotide identity values ranging from 81.85–81.93 with *Methylocystis echinoides* LMG27198, implying that they represent a new species in the genus *Methylocystis*.

DNA isolation, genomic and phylogenetic analyses

High-molecular-weight genomic DNA was extracted using a modified CTAB method[105], from 200 mL amounts of *Methylocella tundrae* T4 grown in methanol, and the *Methylocystis* isolates (strain s IM2, IM3, and IM4) grown in CH_4. The genomes of *Methylocella tundrae* T4 and *Methylocystis* sp. IM3 were sequenced at LabGenomics (Seongnam, Republic of Korea) and Macrogen (Seoul, Republic of Korea) using the PacBio RS II (long-read sequencing) and Illumina HiSeq (2 × 150 bp) platforms, respectively. The genomes of *Methylocystis* sp. IM2 and *Methylocystis* sp. IM4 were sequenced using a MinION R10.4.1 flow cell (FLO-MIN114, Oxford Nanopore Technologies). The PacBio reads were assembled with the Trycycler pipeline (v0.5.4)[106]. Filtered reads were subsampled and assembled using Miniasm/Minpolish (v0.3-r179)[107], Flye (v2.9.2)[108], and Raven (v1.8.3)[109] assemblers. The consensus contigs were polished with Illumina short reads using Polypolish (v0.5.0)[110] and POLCA (v4.0.5)[111]. The circularity was confirmed during the Trycycler pipeline assembly and again by mapping the Illumina reads backward. De novo genome assembly of the MinION long reads was accomplished using Flye (v2.9.2)[108]. Annotation of methanotrophs' genomes was performed with the Prokka annotation pipeline (v1.14.6)[112] and NCBI Prokaryotic Genome Annotation Pipeline (PGAP; v4.2)[113]. Functional assignment of the predicted genes was improved using a set of public databases (InterPro[114], GO[115,116], PFAM[117], CDD[118], TIGRFAM[119], and EggNOG[120]). Prediction of signal peptides and transmembrane helices was performed using the web-based services SignalP (v6.0)[121] and TMHMM (v2.0)[122] with default settings.

The distribution of denitrification genes in methanotroph isolates or metagenome-assembled genomes (MAG) (meeting the following CheckM (v1.2.2) criteria: completeness > 60% and contamination <10%) was examined using genomic data from the NCBI assembly database. Reference protein sequences of denitrification enzymes (NapA, NapB, NarG, NarH, NarI, NirS, NirK, NorB, NorC, and NosZ) were obtained from the NCyc[123] and BV-BRC[124] databases. The annotated protein sequences of methanotrophs were re-annotated against the obtained reference sequences from the NCyc[123] and BV-BRC[124] databases. The identities of the obtained denitrification protein sequences in methanotrophs were verified using manual alignment and tree-building procedures with reference sequences. Sequences incorrectly annotated as denitrification genes were removed, and only candidate genes that clustered with reference sequences were counted as true hits.

For phylogenetic analyses of the NosZ proteins and methanol dehydrogenases of strains T4 and IT6, representative amino acid sequences of the genes of related taxa were obtained from NCBI. The derived amino acid sequences of the NosZ and methanol dehydrogenases (XoxF and MxaF) were aligned using MAFFT (v7.511)[125]. Maximum-likelihood trees were inferred with IQ-TREE (v1.6.12). The constructed trees and operon arrangements were visualized using iTOL (v.6.7.2)[126] and used for annotation. Genomic islands were predicted using the IslandViewer web server[127].

Anoxic growth coupled with N_2O reduction

To demonstrate the ability of N_2OR-containing methanotrophs to grow using N_2O as the electron acceptor, we established anoxic batch cultures of *Methylocella tundrae* T4 and *Methylacidiphilum caldifontis* IT6 in 160-mL bottles containing 20 mL of LSM media and inoculated with 1–5% (v/v) actively growing-cells from the log phase (starting OD_{600} values ≤ 0.05). To remove oxygen, nitrogen gas (N_2, purity >99.999%) was introduced into the bottles via a long needle (18 G). Following that, the bottles were flushed with N_2 gas for 20 min before being sealed with gas-tight butyl rubber stoppers and aluminum crimp seals to prevent O_2 leakage. We used contactless trace-range oxygen sensor spots (TROXSP5) to monitor O_2 contamination (<0.10%, v/v) in the culture bottles incubated after N_2-flushing (see *Analytical methods*, for details). These spots have a detection limit of 20 nM O_2. Chemical-reducing agents, Na_2S (0.5, 1, and 2 mM), cysteine (0.5 mM), DTT (0.5 mM), and titanium citrate (0.5 and 1 mM) in the media resulted in severe cell toxicity, hindering their use in this study as previously reported for N_2OR reducer *Anaeromyxobacter dehalogenans*[128]. When the cultures were incubated without the chemical-reducing agents, the cells completely depleted the trace O_2 concentration present in the culture bottles in less than 24 h as measured by the oxygen sensor spots.

The N_2OR-lacking methanotrophs *Methylocella silvestris* BL2 and *Methylacidiphilum infernorum* IT5, which are closely related to *Methylocella tundrae* T4 and *Methylacidiphilum caldifontis* IT6, respectively, were used as negative controls. Methanol (30 mM), N_2O (5%, v/v), and CO_2 (5%, v/v) were used as the energy source, electron acceptor, and carbon source, respectively. In addition, pyruvate (10 mM) and hydroxyacetone (acetol) (10 mM) were tested as the sole C-C electron donors in strains T4 and IT6, respectively. Furthermore, strain IT6 cells were investigated to grow chemolithoautotrophically in sealed 1-liter bottles (duplicate) containing 20 mL of LSM medium at pH 2.0 on H_2 (10% v/v) with and without N_2O (5% v/v). As part of the control experiments, we incubated cells from the four strains in LSM

media under anoxic conditions (without N_2O) to assess the contribution of the initial trace O_2 present in the culture bottles to biomass increase. The increase in biomass as OD_{600} by the trace O_2 in the control cultures was negligible when compared to cultures growing with N_2O as the sole electron acceptor (see Fig. 2C, F, I, L). Positive control experiments with methanol (30 mM) and O_2 (5%, v/v) as the electron donor and electron acceptor, respectively, were conducted for each strain. The concentrations of H_2, O_2, N_2O, NO_3^-, and NO_2^- were monitored at intervals during incubations (described in *Analytical methods*). Cell growth was also evaluated using optical density measurements (λ = 600 nm), direct microscopic cell counts, and real-time quantification of 16 S rRNA gene abundance (described in *Analytical methods*). All growth experiments were performed in triplicates unless otherwise stated.

Next, we checked the anoxic growth of *Methylocella* strains on NO_3^- (2 to 4 mM KNO_3) as the terminal electron acceptor instead of N_2O. Methanol (30 mM) was used as the sole electron donor and 2 mM NH_4^+ was used as the N-source. To compare the effect of electron donors on NO_3^- and NO_2^- reduction, *Methylocella* strains were also anoxically grown in LSM medium containing a C-C substrate, pyruvate (10 mM). Cells of strain T4 were grown under O_2-replete (O_2; 21%, v/v) or anoxic conditions (O_2; 0%, v/v, N_2O; 5%, v/v) for the NO_2^- toxicity test (triplicates) with varying NO_2^- (KNO_2) concentrations (0, 0.01, 0.03, 0.1, 0.3, and 1 mM).

Analytical methods

A YL 6100 gas chromatograph (YL Instrument Co., Anyang, South Korea) with a flame ionization detector (FID) and a thermal conductivity detector (TCD) was used to analyze the mixing ratios of CH_4, N_2O, and H_2 in the headspace of the sealed bottles used to cultivate the *Methylocella* and *Methylacidiphilum* strains. Using a Hamilton glass syringe, 100 μL of the sealed bottle headspaces were injected into a gas chromatograph equipped with MolSieve 5 A column (3Ft, 1/8, 2 mm, 60/80 SST, Agilent Technologies, Inc., CA, USA; for separating H_2, O_2, and N_2O) and Haysep N column (7Ft, 1/8, 2 mm, 60/80 SST, Agilent Technologies, Inc., CA, USA; for separating CO_2 and CH_4) to determine the gases present. Helium was used as the carrier gas, with a flow rate of 15 mL·min^{-1}. By utilizing pure gases of known concentrations, a calibration curve of the gases used as substrates was generated. The bottles were fitted with contactless trace range oxygen sensor spots (TROXSP5, PyroScience, Germany) calibrated at 0% and ambient air (21% oxygen), and a FireSting-Pro multi-analyte meter (FSPRO-4, PyroScience, Germany) was used to measure the O_2 concentration in the sealed bottles. Acidic Griess reagent and VCl_2/Griess reagent were used for photometric quantification of NO_2^- and NO_3^- concentrations[129], respectively, using a SpectraMax M2 microplate reader (Molecular Devices, USA). Cell growth was assessed by measuring changes in OD_{600} using a spectrophotometer (Optizen 2120UV, Mecasys Co., Daejeon, Korea). Real-time quantification of the 16 S rRNA gene was performed using the 518 F/786 R primer set[130]. The total cell number was determined by counting cells stained with DAPI (4,6-diamidino-2-phenylindole) using an epifluorescence microscope (AxioScope.A1; Carl Zeiss, Oberkochen, Germany).

Kinetic analysis using microrespirometry (MR)

For kinetic analysis using microrespirometry (MR), *Methylocella tundrae* T4 cells were grown under three different O_2 conditions: O_2-replete ($CH_3OH + O_2$), suboxic ($CH_4 + O_2 + N_2O$), and anoxic ($CH_3OH + N_2O$). *Methylacidiphilum caldifontis* IT6 cells were grown under O_2-replete ($CH_3OH + O_2$) and anoxic ($CH_3OH + N_2O$) conditions. The O_2-replete growth conditions included ambient air (21% O_2, v/v) and CH_3OH (30 mM) as the sole electron donor. The suboxic cell cultures were grown under a condition that included CH_4 (5%, v/v) as the sole electron donor and O_2 (0.5%, v/v) with N_2O (1%, v/v) as terminal electron acceptors. O_2 (0.5%, v/v) was resupplied intermittently before its depletion. Anaerobically grown cells were cultured in bottles containing 30 mM CH_3OH as the sole electron donor and 5% (v/v) N_2O as the terminal electron acceptor. The cultures were monitored daily and harvested as soon as active consumption of electron donors and acceptors was detected. After being collected by centrifugation (5000 × *g*, 30 min, 25 °C), the cells were washed twice with substrate- and N-source-free MES-buffered LSM (20 mM MES; pH 5.5) or H_2SO_4-buffered LSM (4 mM H_2SO_4; pH 2.0) and then resuspended in 20 mL of the same media without electron donors and acceptors. In the cultures grown under anoxic and suboxic conditions, the cell suspensions were transferred to sealed 20-mL bottles and flushed with nitrogen gas (N_2, purity >99.999%) before use. The cell suspensions were dispensed into a double-port MR chamber (no headspace) with a capacity of 5 or 10 mL outfitted with O_2 and N_2O-detecting microsensors, two MR injection lids, and two glass-coated stir bars. Kinetics and stoichiometry of N_2O and O_2 reduction coupled to CH_3OH oxidation were estimated using anoxic $CH_3OH + N_2O$- and oxic $CH_3OH + O_2$-grown cells, respectively. Anoxic $CH_3OH + N_2O$-grown cells were used to test CH_3OH-dependent O_2 and N_2O uptake by strains IT6 (starting OD_{600} = 0.96) and T4 (starting OD_{600} = 0.79). The effect of O_2 to N_2OR activities of strains T4 and IT6 was determined by spiking varying O_2 to the N_2O respiring cells. In a 5-mL MR chamber, suboxic $CH_4 + O_2 + N_2O$-grown cells of strain T4 (starting OD_{600} = 1.0) were used to test the CH_4-dependent simultaneous respiration of O_2 and N_2O.

All MR experiments were performed in a recirculating water bath at 27 °C and 50 °C for strains T4 and IT6, respectively. A 10-μL or 50-μL syringe (Hamilton, Reno, USA) fitted with a 26 G needle was used to inject the substrate (CH_4, CH_3OH, N_2O, or O_2) into the chamber via an injection port. Concentrations of O_2 and N_2O were measured using an OX-MR oxygen microsensor (OX-MR-202142, Unisense, Aarhus, Denmark) and a N_2O-MR sensor (N2O-MR-303088, Unisense), respectively. The detection limits of the OX-MR and N_2O-MR microsensors are 0.3 μM O_2 and 0.1 μM N_2O, respectively. The OX-MR and N_2O-MR microsensors were directly plugged into a microsensor multimeter before being polarized for more than a day and calibrated according to the manufacturer's instructions. All data from the microsensor multimeter was logged onto a laptop using SensorTrace Suite software (v.3.3.0, Unisense). Anoxically prepared aliquots of N_2O, CH_4, and CH_3OH were injected into the MR chamber via the injection port with a 10-μL syringe (Hamilton, Reno, USA). Anoxic substrate-free LSM media (at pH 2.0 and 5.5) were prepared by sparging the solutions with N_2 gas for 1 h before use. Anoxic saturated-aqueous CH_4 and N_2O solutions were made in capped 160-mL bottles containing 100 mL of LSM medium and pressurized with CH_4 or N_2O (1, 2, or 3 atm; 100%, v/v). Saturated-aqueous O_2 solutions were prepared in capped 160-mL bottles containing 100 mL of LSM medium and pressurized with O_2 (1, 2, and 3 atm; 100%, v/v).

Growth based on CH_4 oxidation coupled with co-respiration of O_2 and N_2O

Suboxic cultivations were carried out to investigate the growth of *Methylocella tundrae* T4 by oxidizing methane with simultaneous respiration of O_2 and N_2O. The experiments were conducted in N_2-flushed 2-liter sealed bottles containing 60 mL of LSM medium with 2 mM NH_4^+ as the N-source. The headspace of the bottles was composed of CH_4 (5%, v/v), O_2 (0.5%, v/v), N_2O (1%, v/v), and CO_2 (5%, v/v) and supplemented with additional O_2 (~0.5%, v/v) before its depletion. The headspace gas (CH_4, N_2O, and O_2) mixing ratios were monitored at intervals during incubations as described above in *Analytical methods*. To investigate the growth benefits of cells of strain T4 respiring N_2O in tandem with O_2 during CH_4 oxidation, an O_2-replete culture was included for comparison (triplicates). The apparent increase in cell densities of both growth conditions was compared using OD_{600} measurements.

Transcriptome analysis

Cells of strains T4 and IT6 were cultured in 60 mL of LSM medium at pH 5.5 and pH 2.0 in sealed 2-liter bottles (4 or 5 replicates) for transcriptome analyses. Strain T4 cells were cultured under three different O_2 levels, with the first setting being O_2-replete ($CH_4 + O_2$ and $CH_3OH + O_2$), the second being suboxic ($CH_4 + O_2 + N_2O$), and the third being anoxic ($CH_3OH + N_2O$). Strain IT6 was cultivated in O_2-replete $CH_3OH + O_2$ and anoxic $CH_3OH + N_2O$ conditions. Cells were grown anaerobically in bottles containing 30 mM CH_3OH as the sole electron donor and 5% N_2O as the terminal electron acceptor. The O_2-replete growth conditions were made up of ambient air (21% O_2, v/v) with CH_4 (5%, v/v) or CH_3OH (30 mM) serving as the sole electron donor. The suboxic growth conditions were made up of a mixture of CH_4 (5% v/v) as the sole electron donor and O_2 (0.5% v/v) and N_2O (1% v/v) as terminal electron acceptors. Before the depletion of O_2, additional O_2 was resupplied intermittently at a mixing ratio of 0.5% (v/v). Contactless trace-range oxygen sensor spots (TROXSP5) were installed into the culture bottles to monitor O_2 concentration.

The cells were harvested during the mid-exponential phase by centrifugation at 5000 × g for 10 min at 25 °C. Total RNA was extracted from the cells in four replicates using the AllPrep DNA/RNA Mini Kit (Qiagen) according to the manufacturer's protocol. RNA quality was checked with the Agilent 2100 Expert Bioanalyzer (Agilent), and cDNA libraries were prepared from the RNA samples using the Nugen Universal Prokaryotic RNA-Seq Library Preparation Kit. The cDNA libraries were sequenced using NovaSeq6000 (Illumina) at LabGenomics (Seongnam, Korea). Read quality was evaluated with FastQC (v0.11.8)[131]. Trimmomatic (v0.36)[132] was used to trim reads with the options: SLIDINGWINDOW:4:15 LEADING:3 TRAILING:3 MINLEN:38 HEADCROP:13. Reads mapped to strains T4 and IT6 rRNA sequences were removed with SortMeRNA (v4.3.6)[133]. The remaining reads were aligned to the genomes of strains T4 and IT6 using Bowtie2 (v2.4.4)[134], and the reads mapped to each gene were counted using HTSeq (v0.12.3)[135]. Expression values are presented as transcripts per kilobase million (TPM). The statistical analysis of differentially expressed genes was performed using the DESeq2 package in R (v4.3.2). A two-sided Wald test was used to calculate the *p* values, and multiple-comparison adjustments were made using the Benjamini-Hochberg method by default in DESeq2 (v1.40.2).

Reporting summary

Further information on research design is available in the Nature Portfolio Reporting Summary linked to this article.

Data availability

All numerical data used to make the figures is provided in source data. The complete genome sequence of strain T4 was deposited in the National Center for Biotechnology Information (NCBI) GenBank (accession nos. CP139089 (Chromosome), CP139088 (Plasmid 1), and CP139087 (Plasmid 2)). The genomic sequences and genome annotations of *Methylocystis* species (strains IM2, IM3, and IM4) and '*Ca*. Methylotropicum kingii' are available on Figshare (https://doi.org/10.6084/m9.figshare.25521913.v2). All previously sequenced genomes analyzed in this study are available in the NCBI Database with the GenBank accession numbers listed in Supplementary Dataset 1. The whole transcriptome data was deposited in the NCBI BioProject database under the accession number PRJNA1050235. The following are the publicly available databases/datasets used in the study: NCBI NR [https://www.ncbi.nlm.nih.gov/refseq/], BV-BRC, NCyc [https://github.com/qichao1984/NCyc], Pfam [https://pfam.xfam.org/], InterPro [https://www.ebi.ac.uk/interpro/], GO [https://geneontology.org/], CDD, TIGRFAM, and EggNOG [https://tigrfams.jcvi.org/cgi-bin/index.cgi]. Source data are provided with this paper.

References

1. IPCC. Summary for Policymakers. In: *Climate Change 2021 – The Physical Science Basis: Working Group I Contribution to the Sixth Assessment Report of the Intergovernmental Panel on Climate Change* (ed Intergovernmental Panel on Climate C). (Cambridge University Press, 2023).
2. Forster, P. et al. The Earth's Energy Budget, Climate Feedbacks and Climate Sensitivity. In *Climate Change 2021: The Physical Science Basis: Working Group I Contribution to the Sixth Assessment Report of the Intergovernmental Panel on Climate* Change (eds Masson-Delmotte, V., P. Zhai, A. Pirani, S.L. Connors, C. Péan, S. Berger, N. Caud, Y. Chen, L. Goldfarb, M.I. Gomis, M. Huang, K. Leitzell, E. Lonnoy, J.B.R. Matthews, T.K. Maycock, T. Waterfield, O. Yelekçi, R. Yu, and B. Zhou) (Cambridge University Press United Kingdom and New York, NY, USA, 2023).
3. Prinn, R. G. et al. Evidence for variability of atmospheric hydroxyl radicals over the past quarter century. *Geophys. Res. Lett.* **32**, L07809 (2005).
4. Myhre, G. et al. Anthropogenic and natural radiative forcing. in *Climate change 2013: The physical science basis. Contribution of working group I to the fifth assessment report of the Intergovernmental Panel on Climate Change* (eds Stocker T. F., et al.) (Cambridge University Press, 2013).
5. Szopa, S. et al. Short-Lived Climate Forcers. In: *Climate Change 2021: The Physical Science Basis. Contribution of Working Group I to the Sixth Assessment Report of the Intergovernmental Panel on Climate Change* (eds Masson-Delmotte V., et al.) (Cambridge University Press, 2021).
6. Prather, M. J. et al. Measuring and modeling the lifetime of nitrous oxide including its variability. *J. Geophys. Res. Atmos.* **120**, 5693–5705 (2015).
7. Ravishankara, A. R., Daniel, J. S. & Portmann, R. W. Nitrous oxide (N_2O): the dominant ozone-depleting substance emitted in the 21st century. *Science* **326**, 123–125 (2009).
8. Montzka, S. A., Dlugokencky, E. J. & Butler, J. H. Non-CO_2 greenhouse gases and climate change. *Nature* **476**, 43–50 (2011).
9. Canadell, J. G. et al. Global Carbon and Other Biogeochemical Cycles and Feedbacks. In *Climate Change 2021:The Physical Science Basis: Working Group I Contribution to the Sixth Assessment Report of the Intergovernmental Panel on Climate Change* (eds Masson-Delmotte, V., P. Zhai, A. Pirani, S.L. Connors, C. Péan, S. Berger, N. Caud, Y. Chen, L. Goldfarb, M.I. Gomis, M. Huang, K. Leitzell, E. Lonnoy, J.B.R. Matthews, T.K. Maycock, T. Waterfield, O. Yelekçi, R. Yu, and B. Zhou) (Cambridge University Press, 2021).
10. Butterbach-Bahl, K., Baggs, E. M., Dannenmann, M., Kiese, R. & Zechmeister-Boltenstern, S. Nitrous oxide emissions from soils: how well do we understand the processes and their controls? *Philos. Trans. R. Soc. Lond. B Biol. Sci.* **368**, 20130122 (2013).
11. Ringeval, B. et al. Climate-CH_4 feedback from wetlands and its interaction with the climate-CO_2 feedback. *Biogeosciences* **8**, 2137–2157 (2011).
12. Beaulieu, J. J., DelSontro, T. & Downing, J. A. Eutrophication will increase methane emissions from lakes and impoundments during the 21st century. *Nat. Commun.* **10**, 1375 (2019).
13. Murrell, J. C. & Jetten, M. S. The microbial methane cycle. *Environ. Microbiol. Rep.* **1**, 279–284 (2009).
14. Conrad, R. The global methane cycle: recent advances in understanding the microbial processes involved. *Environ. Microbiol. Rep.* **1**, 285–292 (2009).
15. Bürgmann, H. Methane oxidation (aerobic). in *Encyclopedia of Geobiology*, (eds Reitner, J., Thiel, V.) (Springer Netherlands, 2011).
16. Leu, A. O. et al. Anaerobic methane oxidation coupled to manganese reduction by members of the *Methanoperedenaceae*. *ISME J.* **14**, 1030–1041 (2020).

17. Haroon, M. F. et al. Anaerobic oxidation of methane coupled to nitrate reduction in a novel archaeal lineage. *Nature* **500**, 567 (2013).
18. Scheller, S., Yu, H., Chadwick, G. L., McGlynn, S. E. & Orphan, V. J. Artificial electron acceptors decouple archaeal methane oxidation from sulfate reduction. *Science* **351**, 703–707 (2016).
19. Ettwig, K. F. et al. Archaea catalyze iron-dependent anaerobic oxidation of methane. *Proc. Natl Acad. Sci. USA* **113**, 12792–12796 (2016).
20. Ettwig, K. F. et al. Nitrite-driven anaerobic methane oxidation by oxygenic bacteria. *Nature* **464**, 543–548 (2010).
21. Kits, K. D., Campbell, D. J., Rosana, A. R. & Stein, L. Y. Diverse electron sources support denitrification under hypoxia in the obligate methanotroph *Methylomicrobium album* strain BG8. *Front. Microbiol.* **6**, 1072–1072 (2015).
22. Kits, K. D., Klotz, M. G. & Stein, L. Y. Methane oxidation coupled to nitrate reduction under hypoxia by the Gammaproteobacterium *Methylomonas denitrificans*, sp. nov. type strain FJG1. *Environ. Microbiol.* **17**, 3219–3232 (2015).
23. Dam, B., Kube, M., Dam, S., Reinhardt, R. & Liesack, W. Complete sequence analysis of two methanotroph-specific repABC-containing plasmids from *Methylocystis* sp. strain SC2. *Appl. Environ. Microbiol.* **78**, 4373–4379 (2012).
24. Kox, M. A. R. et al. Complete genome sequence of the aerobic facultative methanotroph *Methylocella tundrae* strain T4. *Microbiol. Resour. Announc.* **8**, e00286–00219 (2019).
25. Tian, H. et al. A comprehensive quantification of global nitrous oxide sources and sinks. *Nature* **586**, 248–256 (2020).
26. Thomson, A. J., Giannopoulos, G., Pretty, J., Baggs, E. M. & Richardson, D. J. Biological sources and sinks of nitrous oxide and strategies to mitigate emissions. *Philos. Trans. R. Soc. Lond. B Biol. Sci.* **367**, 1157–1168 (2012).
27. Buessecker, S. et al. Coupled abiotic-biotic cycling of nitrous oxide in tropical peatlands. *Nat. Ecol. Evol.* **6**, 1881–1890 (2022).
28. Su, Q., Domingo-Félez, C., Jensen, M. M. & Smets, B. F. Abiotic nitrous oxide (N_2O) production Is strongly pH dependent, but contributes little to overall N_2O emissions in biological nitrogen removal systems. *Environ. Sci. Technol.* **53**, 3508–3516 (2019).
29. Zumft, W. G. & Kroneck, P. M. Respiratory transformation of nitrous oxide (N_2O) to dinitrogen by Bacteria and Archaea. *Adv. Microb. Physiol.* **52**, 107–227 (2007).
30. Graf, D. R., Jones, C. M. & Hallin, S. Intergenomic comparisons highlight modularity of the denitrification pathway and underpin the importance of community structure for N_2O emissions. *PLOS ONE* **9**, e114118 (2014).
31. Sanford, R. A. et al. Unexpected nondenitrifier nitrous oxide reductase gene diversity and abundance in soils. *Proc. Natl Acad. Sci. USA* **109**, 19709–19714 (2012).
32. Hallin, S., Philippot, L., Löffler, F. E., Sanford, R. A. & Jones, C. M. Genomics and ecology of novel N_2O-reducing microorganisms. *Trends Microbiol.* **26**, 43–55 (2018).
33. Payne, W. J., Grant, M. A., Shapleigh, J. & Hoffman, P. Nitrogen oxide reduction in *Wolinella succinogenes* and *Campylobacter* species. *J. Bacteriol.* **152**, 915–918 (1982).
34. Yoon, S., Nissen, S., Park, D., Sanford, R. A. & Löffler, F. E. Nitrous oxide reduction kinetics distinguish bacteria harboring clade I NosZ from those harboring clade II NosZ. *Appl. Environ. Microbiol.* **82**, 3793–3800 (2016).
35. Park, D., Kim, H. & Yoon, S. Nitrous oxide reduction by an obligate aerobic bacterium, *Gemmatimonas aurantiaca* strain T-27. *Appl. Environ. Microbiol.* **83**, e00502–00517 (2017).
36. Dam, B., Dam, S., Blom, J. & Liesack, W. Genome analysis coupled with physiological studies reveals a diverse nitrogen metabolism in *Methylocystis* sp. strain SC2. *PLOS ONE* **8**, e74767 (2013).
37. Knief, C. Diversity and habitat preferences of cultivated and uncultivated aerobic methanotrophic bacteria evaluated based on *pmoA* as molecular marker. *Front. Microbiol.* **6**, 1346 (2015).
38. Reim, A., Lüke, C., Krause, S., Pratscher, J. & Frenzel, P. One millimetre makes the difference: high-resolution analysis of methane-oxidizing bacteria and their specific activity at the oxic–anoxic interface in a flooded paddy soil. *ISME J.* **6**, 2128–2139 (2012).
39. Farhan Ul Haque, M., Crombie, A. T. & Murrell, J. C. Novel facultative *Methylocella* strains are active methane consumers at terrestrial natural gas seeps. *Microbiome* **7**, 134 (2019).
40. Kantor, R. S., Miller, S. E. & Nelson, K. L. The water microbiome through a pilot scale advanced treatment facility for direct potable reuse. *Front. Microbiol.* **10**, 993 (2019).
41. McGuirl, M. A., Bollinger, J. A., Cosper, N., Scott, R. A. & Dooley, D. M. Expression, purification, and characterization of NosL, a novel Cu(I) protein of the nitrous oxide reductase (nos) gene cluster. *J. Biol. Inorg. Chem.* **6**, 189–195 (2001).
42. Kang, C. S., Dunfield, P. F. & Semrau, J. D. The origin of aerobic methanotrophy within the *Proteobacteria*. *FEMS Microbiol. Lett.* **366**, fnz096 (2019).
43. Berks, B. C., Palmer, T. & Sargent, F. Protein targeting by the bacterial twin-arginine translocation (Tat) pathway. *Curr. Opin. Microbiol.* **8**, 174–181 (2005).
44. Awala, S. I. et al. Verrucomicrobial methanotrophs grow on diverse C3 compounds and use a homolog of particulate methane monooxygenase to oxidize acetone. *ISME J.* **15**, 3636–3647 (2021).
45. Zhang, L., Trncik, C., Andrade, S. L. A. & Einsle, O. The flavinyl transferase ApbE of *Pseudomonas stutzeri* matures the NosR protein required for nitrous oxide reduction. *Biochim. Biophys. Acta Bioenerg.* **1858**, 95–102 (2017).
46. Honisch, U. & Zumft, W. G. Operon structure and regulation of the nos gene region of Pseudomonas stutzeri, encoding an ABC-Type ATPase for maturation of nitrous oxide reductase. *J. Bacteriol.* **185**, 1895–1902 (2003).
47. Simon, J., Einsle, O., Kroneck, P. M. & Zumft, W. G. The unprecedented nos gene cluster of *Wolinella succinogenes* encodes a novel respiratory electron transfer pathway to cytochrome c nitrous oxide reductase. *FEBS Lett.* **569**, 7–12 (2004).
48. Suzuki, M., Cui, Z. J., Ishii, M. & Igarashi, Y. Nitrate respiratory metabolism in an obligately autotrophic hydrogen-oxidizing bacterium, *Hydrogenobacter thermophilus* TK-6. *Arch. Microbiol.* **175**, 75–78 (2001).
49. Sharp, C. E., den Camp, H.J.M.O., Tamas, I., Dunfield P. F. Unusual members of the PVC superphylum: the methanotrophic Verrucomicrobia genus "Methylacidiphilum". in *Planctomycetes: cell structure, origins and biology* (ed Fuerst, J. A.) (Humana Press, 2013).
50. Bay, S. K. et al. Trace gas oxidizers are widespread and active members of soil microbial communities. *Nat. Microbiol.* **6**, 246–256 (2021).
51. Dedysh, S. N., Knief, C. & Dunfield, P. F. *Methylocella* species are facultatively methanotrophic. *J. Bacteriol.* **187**, 4665–4670 (2005).
52. Awala, S. I. et al. *Methylacidiphilum caldifontis* gen. nov., sp. nov., a thermoacidophilic methane-oxidizing bacterium from an acidic geothermal environment, and descriptions of the family *Methylacidiphilaceae* fam. nov. and order *Methylacidiphilales* ord. nov. *Int. J. Syst. Evol. Microbiol.* **73**, 006085 (2023).
53. Thauer, R. K., Jungermann, K. & Decker, K. Energy conservation in chemotrophic anaerobic bacteria. *Bacteriol. Rev.* **41**, 100–180 (1977).
54. Svensson-Ek, M. et al. The X-ray crystal structures of wild-type and EQ (I-286) mutant cytochrome c oxidases from *Rhodobacter sphaeroides*. *J. Mol. Biol.* **321**, 329–339 (2002).

55. Iwata, S., Ostermeier, C., Ludwig, B. & Michel, H. Structure at 2.8 Å resolution of cytochrome c oxidase from *Paracoccus denitrificans*. *Nature* **376**, 660–669 (1995).
56. Chen, J. & Strous, M. Denitrification and aerobic respiration, hybrid electron transport chains and co-evolution. *Biochim. Biophys. Acta Bioenerg.* **1827**, 136–144 (2013).
57. Bergaust, L., Mao, Y., Bakken, L. R. & Frostegård, A. Denitrification response patterns during the transition to anoxic respiration and posttranscriptional effects of suboptimal pH on nitrous oxide reductase in *Paracoccus denitrificans*. *Appl. Environ. Microbiol.* **76**, 6387–6396 (2010).
58. Van den Heuvel, R. N., Bakker, S. E., Jetten, M. S. & Hefting, M. M. Decreased N_2O reduction by low soil pH causes high N_2O emissions in a riparian ecosystem. *Geobiology* **9**, 294–300 (2011).
59. Palmer, K., Drake, H. L. & Horn, M. A. Association of novel and highly diverse acid-tolerant denitrifiers with N_2O fluxes of an acidic fen. *Appl. Environ. Microbiol.* **76**, 1125–1134 (2010).
60. Brenzinger, K., Dörsch, P. & Braker, G. pH-driven shifts in overall and transcriptionally active denitrifiers control gaseous product stoichiometry in growth experiments with extracted bacteria from soil. *Front. Microbiol.* **6**, 961 (2015).
61. Lycus, P. et al. Phenotypic and genotypic richness of denitrifiers revealed by a novel isolation strategy. *ISME J.* **11**, 2219–2232 (2017).
62. Almeida, J. S., Júlio, S. M., Reis, M. A. & Carrondo, M. J. Nitrite inhibition of denitrification by *Pseudomonas fluorescens*. *Biotechnol. Bioeng.* **46**, 194–201 (1995).
63. Fang, F. C. Antimicrobial reactive oxygen and nitrogen species: concepts and controversies. *Nat. Rev. Microbiol.* **2**, 820–832 (2004).
64. Bueno, E., Sit, B., Waldor, M. K. & Cava, F. Anaerobic nitrate reduction divergently governs population expansion of the enteropathogen *Vibrio cholerae*. *Nat. Microbiol.* **3**, 1346–1353 (2018).
65. Vadivelu, V. M., Keller, J. & Yuan, Z. Free ammonia and free nitrous acid inhibition on the anabolic and catabolic processes of *Nitrosomonas* and *Nitrobacter*. *Water Sci Technol.* **56**, 89–97 (2007).
66. Zhu-Barker, X., Cavazos, A. R., Ostrom, N. E., Horwath, W. R. & Glass, J. B. The importance of abiotic reactions for nitrous oxide production. *Biogeochemistry* **126**, 251–267 (2015).
67. Cole, J. Anaerobic bacterial response to nitric oxide stress: Widespread misconceptions and physiologically relevant responses. *Mol. Microbiol.* **116**, 29–40 (2021).
68. Auclair, J., Lépine, F., Parent, S. & Villemur, R. Dissimilatory reduction of nitrate in seawater by a *Methylophaga* strain containing two highly divergent narG sequences. *ISME J.* **4**, 1302–1313 (2010).
69. Kamps, J. J., Hopkinson, R. J., Schofield, C. J. & Claridge, T. D. How formaldehyde reacts with amino acids. *Commun. Chem.* **2**, 126 (2019).
70. Dedysh, S. N. & Dunfield, P. F. Facultative and obligate methanotrophs:how to identify and differentiate them.*Methods Enzymol.* **495**, 31–44 (2011).
71. Purchase, M. L., Bending, G. D. & Mushinski, R. M. Spatiotemporal variations of soil reactive nitrogen oxide fluxes across the anthropogenic landscape. *Environ. Sci. Technol.* **57**, 16348–16360 (2023).
72. Pauleta, S. R., Dell'Acqua, S. & Moura, I. Nitrous oxide reductase. *Coord. Chem. Rev.* **257**, 332–349 (2013).
73. Wang, Z., Vishwanathan, N., Kowaliczko, S. & Ishii, S. Clarifying microbial nitrous oxide reduction under aerobic conditions: tolerant, intolerant, and sensitive. *Microbiol. Spectr.* **11**, e0470922 (2023).
74. Suenaga, T., Riya, S., Hosomi, M. & Terada, A. Biokinetic characterization and activities of N_2O-reducing bacteria in response to various oxygen levels. *Front. Microbiol.* **9**, 697 (2018).
75. Hilgeri, H. & Humer, M. Biotic landfill cover treatments for mitigating methane emissions. *Environ. Monit. Assess.* **84**, 71–84 (2003).
76. Ross, M. O. & Rosenzweig, A. C. A tale of two methane monooxygenases. *J. Biol. Inorg. Chem.* **22**, 307–319 (2017).
77. Hein, S., Witt, S. & Simon, J. Clade II nitrous oxide respiration of *Wolinella succinogenes* depends on the NosG, -C1, -C2, -H electron transport module, NosB and a Rieske/cytochrome bc complex. *Environ. Microbiol.* **19**, 4913–4925 (2017).
78. Keltjens, J. T., Pol, A., Reimann, J. & Op den Camp, H. J. M. PQQ-dependent methanol dehydrogenases: rare-earth elements make a difference. *Appl. Microbiol. Biotechnol.* **98**, 6163–6183 (2014).
79. Sirota, F. L., Maurer-Stroh, S., Li, Z., Eisenhaber, F. & Eisenhaber, B. Functional classification of super-large families of enzymes based on substrate binding pocket residues for biocatalysis and enzyme engineering applications. *Front. Bioeng. Biotechnol.* **9**, 701120 (2021).
80. Le, T.-K., Lee, Y.-J., Han, G. H. & Yeom, S.-J. Methanol dehydrogenases as a key biocatalysts for synthetic methylotrophy. *Front. Bioeng. Biotechnol.* **9**, 787791 (2021).
81. Bonnot, F., Iavarone, A. T. & Klinman, J. P. Multistep, eight-electron oxidation catalyzed by the cofactorless oxidase, PqqC: identification of chemical intermediates and their dependence on molecular oxygen. *Biochemistry* **52**, 4667–4675 (2013).
82. Matsushita, K. et al. *Escherichia coli* is unable to produce pyrroloquinoline quinone (PQQ). *Microbiology* **143**, 3149–3156 (1997).
83. Zhang, W. et al. Guidance for engineering of synthetic methylotrophy based on methanol metabolism in methylotrophy. *RSC Adv.* **7**, 4083–4091 (2017).
84. Chu, F. & Lidstrom, M. E. XoxF Acts as the predominant methanol dehydrogenase in the type I methanotroph *Methylomicrobium buryatense*. *J .Bacteriol.* **198**, 1317–1325 (2016).
85. Kim, H. J. & Graham, D. W. Effect of oxygen level on simultaneous nitrogenase and sMMO expression and activity in *Methylosinus trichosporium* OB3b and its $sMMO^C$ mutant, PP319: aerotolerant N_2 fixation in PP319. *FEMS Microbiol. Lett.* **201**, 133–138 (2001).
86. Kim, H. J. & Graham, D. W. Effects of oxygen and nitrogen conditions on the transformation kinetics of 1,2-dichloroethenes by *Methylosinus trichosporium* OB3b and its $sMMO^C$ mutant. *Biodegradation* **14**, 407–414 (2003).
87. Smirnova, A. V. & Dunfield, P. F. Differential transcriptional activation of genes encoding soluble methane monooxygenase in a facultative versus an obligate methanotroph. *Microorganisms* **6**, 20 (2018).
88. Theisen, A. R. et al. Regulation of methane oxidation in the facultative methanotroph *Methylocella silvestris* BL2. *Mol. Microbiol.* **58**, 682–692 (2005).
89. Reimer, L. C., Sarda Carbasse, J., Koblitz, J., Podstawka, A. & Overmann, J. *Methylocella tundrae* Dedysh et al. 2004. DSMZ. https://doi.org/10.13145/bacdive1659.20230509.8.1 (2023).
90. Reimer, L. C., Sarda Carbasse, J., Koblitz J., Podstawka, A., Overmann, J. *Methylocystis echinoides* (ex Gal'chenko et al. 1977) DSMZ. https://doi.org/10.13145/bacdive169085.20230509.8.1 (2023).
91. Qian, H. et al. Greenhouse gas emissions and mitigation in rice agriculture. *Nat. Rev. Earth Environ.* **4**, 716–732 (2023).
92. Kolb, S. & Horn, M. A. Microbial CH_4 and N_2O consumption in acidic wetlands. *Front. Microbiol.* **3**, 78 (2012).
93. Ishii, S., Ohno, H., Tsuboi, M., Otsuka, S. & Senoo, K. Identification and isolation of active N_2O reducers in rice paddy soil. *ISME J.* **5**, 1936–1945 (2011).
94. Taminskas, J. et al. Climate change and water table fluctuation: Implications for raised bog surface variability. *Geomorphology* **304**, 40–49 (2018).
95. Ratcliffe, J. L., Campbell, D. I., Clarkson, B. R., Wall, A. M. & Schipper, L. A. Water table fluctuations control CO_2 exchange in

wet and dry bogs through different mechanisms. *Sci. Total Environ.* **655**, 1037–1046 (2019).
96. Evans, C. D. et al. Overriding water table control on managed peatland greenhouse gas emissions. *Nature* **593**, 548–552 (2021).
97. Kotsyurbenko O. R., Glagolev M. V., Merkel A. Y., Sabrekov A. F., Terentieva I. E. Methanogenesis in Soils, Wetlands, and Peat. in *Biogenesis of Hydrocarbons* (eds Stams A. J. M., Sousa D. Z.) (Springer International Publishing, 2019).
98. Angle, J. C. et al. Methanogenesis in oxygenated soils is a substantial fraction of wetland methane emissions. *Nat. Commun.* **8**, 1567 (2017).
99. Zhu, X., Burger, M., Doane, T. A. & Horwath, W. R. Ammonia oxidation pathways and nitrifier denitrification are significant sources of N_2O and NO under low oxygen availability. *Proc. Natl Acad. Sci. USA* **110**, 6328–6333 (2013).
100. Hakobyan, A., Zhu, J., Glatter, T., Paczia, N. & Liesack, W. Hydrogen utilization by *Methylocystis* sp. strain SC2 expands the known metabolic versatility of type IIa methanotrophs. *Metab. Eng.* **61**, 181–196 (2020).
101. Widdel, F., Bak, F. Gram-negative mesophilic sulfate-reducing bacteria. In *The Prokaryotes: A Handbook on the Biology of Bacteria: Ecophysiology, Isolation, Identification, Applications* (eds Balows, A., Trüper, H. G., Dworkin, M., Harder, W., Schleifer, K.-H.) (Springer International Publishing, 1992).
102. Bellosillo, L. A. Effects of environmental factors on methanotroph communities from a forest soil, lake sediment and a landfill soil. (Chungbuk National University, 2020).
103. Awala, S. I. et al. *Methylococcus geothermalis* sp. nov., a methanotroph isolated from a geothermal field in the Republic of Korea. *Int. J. Syst. Evol. Microbiol.* **70**, 5520–5530 (2020).
104. Weisburg, W. G., Barns, S. M., Pelletier, D. A. & Lane, D. J. 16S ribosomal DNA amplification for phylogenetic study. *J. Bacteriol.* **173**, 697–703 (1991).
105. Hurt, R. A. et al. Simultaneous recovery of RNA and DNA from soils and sediments. *Appl. Environ. Microbiol.* **67**, 4495–4503 (2001).
106. Wick, R. R. et al. Trycycler: consensus long-read assemblies for bacterial genomes. *Genome Biol.* **22**, 266 (2021).
107. Li, H. Minimap and miniasm: fast mapping and de novo assembly for noisy long sequences. *Bioinformatics* **32**, 2103–2110 (2016).
108. Kolmogorov, M., Yuan, J., Lin, Y. & Pevzner, P. A. Assembly of long, error-prone reads using repeat graphs. *Nat. Biotechnol.* **37**, 540–546 (2019).
109. Vaser, R. & Šikić, M. Time- and memory-efficient genome assembly with Raven. *Nat. Comput. Sci.* **1**, 332–336 (2021).
110. Wick, R. R. & Holt, K. E. Polypolish: short-read polishing of long-read bacterial genome assemblies. *PLoS Comput. Biol.* **18**, e1009802 (2022).
111. Zimin, A. V. & Salzberg, S. L. The genome polishing tool POLCA makes fast and accurate corrections in genome assemblies. *PLoS Comput. Biol.* **16**, e1007981 (2020).
112. Seemann, T. Prokka: rapid prokaryotic genome annotation. *Bioinformatics* **30**, 2068–2069 (2014).
113. Tatusova, T. et al. NCBI prokaryotic genome annotation pipeline. *Nucleic Acids Res.* **44**, 6614–6624 (2016).
114. Hunter, S. et al. InterPro: the integrative protein signature database. *Nucleic Acids Res.* **37**, D211–D215 (2009).
115. Ashburner, M. et al. Gene ontology: tool for the unification of biology. *Nat. Genet.* **25**, 25–29 (2000).
116. Consortium, T. G. O. The gene ontology resource: enriching a GOld mine. *Nucleic Acids Res.* **49**, D325–d334 (2021).
117. Finn, R. D. et al. Pfam: the protein families database. *Nucleic Acids Res.* **42**, D222–D230 (2014).
118. Lu, S. et al. CDD/SPARCLE: the conserved domain database in 2020. *Nucleic Acids Res.* **48**, D265–d268 (2020).
119. Haft, D. H., Selengut, J. D. & White, O. The TIGRFAMs database of protein families. *Nucleic Acids Res.* **31**, 371–373 (2003).
120. Huerta-Cepas, J. et al. eggNOG 5.0: a hierarchical, functionally and phylogenetically annotated orthology resource based on 5090 organisms and 2502 viruses. *Nucleic Acids Res.* **47**, D309–D314 (2019).
121. Almagro Armenteros, J. J. et al. SignalP 5.0 improves signal peptide predictions using deep neural networks. *Nat. Biotechnol.* **37**, 420–423 (2019).
122. Krogh, A., Larsson, B., von Heijne, G. & Sonnhammer, E. L. Predicting transmembrane protein topology with a hidden Markov model: application to complete genomes. *J. Mol. Biol.* **305**, 567–580 (2001).
123. Tu, Q., Lin, L., Cheng, L., Deng, Y. & He, Z. NCycDB: a curated integrative database for fast and accurate metagenomic profiling of nitrogen cycling genes. *Bioinformatics* **35**, 1040–1048 (2018).
124. Olson, R. D. et al. Introducing the bacterial and viral Bioinformatics Resource Center (BV-BRC): a resource combining PATRIC, IRD and ViPR. *Nucleic Acids Res.* **51**, D678–D689 (2022).
125. Katoh, K. & Standley, D. M. MAFFT multiple sequence alignment software version 7: improvements in performance and usability. *Mol. Biol. Evol.* **30**, 772–780 (2013).
126. Letunic, I. & Bork, P. Interactive Tree Of Life (iTOL) v5: an online tool for phylogenetic tree display and annotation. *Nucleic Acids Res.* **49**, W293–W296 (2021).
127. Bertelli, C. et al. IslandViewer 4: expanded prediction of genomic islands for larger-scale datasets. *Nucleic Acids Res.* **45**, W30–w35 (2017).
128. Onley, J. R., Ahsan, S., Sanford, R. A. & Löffler, F. E. Denitrification by *Anaeromyxobacter dehalogenans*, a common soil bacterium lacking the nitrite reductase genes *nirS* and *nirK*. *Appl. Environ. Microbiol.* **84**, e01985–01917 (2018).
129. Miranda, K. M., Espey, M. G. & Wink, D. A. A rapid, simple spectrophotometric method for simultaneous detection of nitrate and nitrite. *Nitric Oxide* **5**, 62–71 (2001).
130. Muyzer, G., De Waal, E. C. & Uitterlinden, A. G. Profiling of complex microbial populations by denaturing gradient gel electrophoresis analysis of polymerase chain reaction-amplified genes coding for 16S rRNA. *Appl. Environ. Microbiol.* **59**, 695–700 (1993).
131. Andrews, S. FastQC: a quality control tool for high throughput sequence data http://www.bioinformatics.babraham.ac.uk/projects/fastqc (2010).
132. Bolger, A. M., Lohse, M. & Usadel, B. Trimmomatic: a flexible trimmer for Illumina sequence data. *Bioinformatics* **30**, 2114–2120 (2014).
133. Kopylova, E., Noé, L. & Touzet, H. SortMeRNA: fast and accurate filtering of ribosomal RNAs in metatranscriptomic data. *Bioinformatics* **28**, 3211–3217 (2012).
134. Langmead, B. & Salzberg, S. L. Fast gapped-read alignment with Bowtie 2. *Nat. Methods* **9**, 357–359 (2012).
135. Anders, S., Pyl, P. T. & Huber, W. HTSeq—a Python framework to work with high-throughput sequencing data. *Bioinformatics* **31**, 166–169 (2014).
136. Hein, S. & Simon, J. Bacterial nitrous oxide respiration: electron transport chains and copper transfer reactions. *Adv .Microb. Physiol.* **75**, 137–175 (2019).
137. Torres, M. J. et al. Nitrous oxide metabolism in nitrate-reducing bacteria: physiology and regulatory mechanisms. *Adv. Microb. Physiol.* **68**, 353–432 (2016).

Acknowledgements

This work was supported by the NRF (National Research Foundation of Korea) grant funded by the Korean government (Ministry of Science and ICT) (2021R1A2C3004015), the Basic Science Research Program through NRF funded by the Ministry of Education (2020R1A6A1A06046235), and

the National Institute of Agricultural Science, Ministry of Rural Development Administration, Republic of Korea (research project PJ01700703). J.-H.G. was supported by the NRF grant funded by the Korean government (Ministry of Science and ICT) (RS-2023-00213601). M.-Y.J. was supported by the NRF grant funded by the Korean government (Ministry of Science and ICT) (2021R1C1C1008303 and 2022R1A4A503144711). P.F.D. was supported by a Natural Sciences and Engineering Research Council of Canada (NSERC) Discovery Grant (2019-06265). M.W. was supported by the Austrian Science Fund FWF Cluster of Excellence "Microbiomes drive planetary health" COE7.

Author contributions

S.I.A., J.-H.G., and S.-K.R. designed research. S.I.A., J.-H.G., M.-Y.J., and Y.K. performed research. S.I.A., J.-H.G., Y.K., M.-Y.J., P.F.D., and S.-K.R. analyzed data. S.I.A., J.-H.G., M.-Y.J., P.F.D., M.W., and S.-K.R. wrote the manuscript with contributions and comments from all co-authors.

Competing interests

The authors declare no competing interests.

Additional information

Supplementary information The online version contains supplementary material available at https://doi.org/10.1038/s41467-024-48161-z.

Correspondence and requests for materials should be addressed to Sung-Keun Rhee.

Peer review information *Nature Communications* thanks Simon Guerrero-Cruz, Lisa Stein and the other, anonymous, reviewer for their contribution to the peer review of this work. A peer review file is available.